การพัฒนาเซลลูโลสจากแบคทีเรียเพื่อใช้เป็นตัวรองรับของตัวเร่งปฏิกิริยาอะลูมินาสำหรับการขจัดน้ำของเอทานอล

นายมิฟตะห์ฟาริด อิบนูอับดุลวาฮับ

วิทยานิพนธ์นี้เป็นส่วนหนึ่งของการศึกษาตามหลักสูตรปริญญาวิศวกรรมศาสตรมหาบัณฑิต
สาขาวิชาวิศวกรรมเคมี ภาควิชาวิศวกรรมเคมี
คณะวิศวกรรมศาสตร์ จุฬาลงกรณ์มหาวิทยาลัย
ปีการศึกษา 2557

DEVELOPMENT OF BACTERIAL CELLULOSE AS ALUMINA CATALYST SUPPORT FOR ETHANOL DEHYDRATION

Mr. Miftahfarid Ibnu Abdulwahab

A Thesis Submitted in Partial Fulfillment of the Requirements

for the Degree of Master of Engineering Program in Chemical Engineering

Department of Chemical Engineering

Faculty of Engineering

Chulalongkorn University

Academic Year 2014

Thesis Title	DEVELOPMENT OF BACTERIAL CELLULOSE AS ALUMINA CATALYST SUPPORT FOR ETHANOL DEHYDRATION
By	Mr. Miftahfarid Ibnu Abdulwahab
Field of Study	Chemical Engineering
Thesis Advisor	Associate Professor Muenduen Phisalaphong, Ph.D.
Thesis Co-Advisor	Associate Professor Bunjerd Jongsomjit, Ph.D.

Accepted by the Faculty of Engineering, Chulalongkorn University in Partial Fulfillment of the Requirements for the Master's Degree

.....Dean of the Faculty of Engineering

(Professor Bundhit Eua-arporn, Ph.D.)

THESIS COMMITTEE

.....Chairman

(Associate Professor Artiwan Shotipruk, Ph.D.)

.....Thesis Advisor

(Associate Professor Muenduen Phisalaphong, Ph.D.)

.....Thesis Co-Advisor

(Associate Professor Bunjerd Jongsomjit, Ph.D.)

.....Examiner

(Associate Professor Joongjai Panpranot, Ph.D.)

.....External Examiner

(Narongsak Chaiyasit, Ph.D.)

มิฟตะห์ฟาริด อิบนูอับดุลวาฮับ : การพัฒนาเซลลูโลสจากแบคทีเรียเพื่อใช้เป็นตัวรองรับของตัวเร่งปฏิกิริยาอะลูมินาสำหรับการขจัดน้ำของเอทานอล (DEVELOPMENT OF BACTERIAL CELLULOSE AS ALUMINA CATALYST SUPPORT FOR ETHANOL DEHYDRATION) อ.ที่ปรึกษาวิทยานิพนธ์หลัก: รศ. ดร.เหมือนเดือน พิศาลพงศ์, อ.ที่ปรึกษาวิทยานิพนธ์ร่วม: รศ. ดร.บรรเจิด จงสมจิตร, 72 หน้า.

งานวิจัยนี้ได้พัฒนาตัวรองรับของตัวเร่งปฏิกิริยาอะลูมินาแบบใหม่ที่ทำมาจากเซลลูโลสจากแบคทีเรีย ซึ่งประกอบด้วยเส้นใยเซลลูโลสขนาดนาโนที่สร้างโดยแบคทีเรียชนิด *Acetobactor xylinum* ตัวเร่งปฏิกิริยาอะลูมินาบนตัวรองรับเซลลูโลสดังกล่าวถูกเตรียมโดยการแช่เซลลูโลสจากแบคทีเรียบริสุทธิ์ในรูปไฮโดรเจลลงในสารละลายอะลูมิเนียมไนเตรต จากนั้นทำให้แห้ง ทำการศึกษาผลกระทบของความเข้มข้นของปริมาณโลหะที่เป็นกรด (อะลูมิเนียม) บนตัวรองรับและวิธีการทำให้แห้ง (ทำให้แห้งแบบใช้อากาศร้อนและทำให้แห้งแบบเยือกแข็ง) ที่มีต่อคุณลักษณะของตัวเร่งปฏิกิริยา การวิเคราะห์คุณลักษณะของตัวเร่งปฏิกิริยาอะลูมินาบนตัวรองรับเซลลูโลสจากแบคทีเรียประกอบด้วย การกระเจิงรังสีเอ็กซ์ การดูดซับทางกายภาพด้วยไนโตรเจน กล้องจุลทรรศน์แบบส่องกราด การวิเคราะห์หาชนิดและปริมาณสารโดยการวัดการดูดกลืนแสงของสารในช่วงอินฟาร์เรด การไทเทรตแบบย้อนกลับ และการวิเคราะห์การเปลี่ยนแปลงน้ำหนักโดยใช้ความร้อน หลังจากนั้น ทำการทดสอบความว่องไวของตัวเร่งปฏิกิริยาสำหรับการผลิตเอทิลีนโดยปฏิกิริยาการขจัดน้ำของเอทานอลในวัฏภาคแก๊สที่ความดันบรรยากาศและอุณหภูมิระหว่าง 200 ถึง 400 องศาเซลเซียส จากการศึกษาพบว่า ปริมาณอะลูมิเนียมบนตัวรองรับมีผลกระทบต่อพื้นที่ผิวและความเป็นกรดของตัวเร่งปฏิกิริยา การเพิ่มปริมาณอะลูมิเนียมบนตัวรองรับมีผลทำให้พื้นที่ผิวลดลง แต่คุณสมบัติความเป็นกรดเพิ่มขึ้น ในการศึกษานี้ ตัวเร่งปฏิกิริยาอะลูมินาบนตัวรองรับเซลลูโลสจากแบคทีเรียที่มีปริมาณอะลูมินาร้อยละ 50 และทำให้แห้งแบบใช้อากาศร้อน (50Al/BC-TD) ให้ค่าการเลือกเกิดของเอทิลีนและการเปลี่ยนแปลงของเอทานอลสูงสุดที่อุณหภูมิปฏิกิริยา 400 องศาเซลเซียส

ภาควิชา วิศวกรรมเคมี ลายมือชื่อนิสิต .....

สาขาวิชา วิศวกรรมเคมี ลายมือชื่อ อ.ที่ปรึกษาหลัก .....

ปีการศึกษา 2557 ลายมือชื่อ อ.ที่ปรึกษาร่วม .....

5570936821 : MAJOR CHEMICAL ENGINEERING

KEYWORDS: BACTERIAL CELLULOSE / ACETOBACTER XYLINUM / ETHANOL DEHYDRATION / ALUMINA CATALYST / CATALYST SUPPORT

MIFTAHFARID IBNU ABDULWAHAB: DEVELOPMENT OF BACTERIAL CELLULOSE AS ALUMINA CATALYST SUPPORT FOR ETHANOL DEHYDRATION. ADVISOR: ASSOC. PROF. MUENDUEN PHISALAPHONG, Ph.D., CO-ADVISOR: ASSOC. PROF. BUNJERD JONGSOMJIT, Ph.D., 72 pp.

In this study, novel alumina catalyst support derived from bacterial cellulose (BC) was developed. BC is composed of nanosized cellulose fibers produced by *Acetobacter xylinum*. BC supported alumina catalysts were prepared by soaking purified BC hydrogel in aluminium nitrate aqueous solution and then dehydrating. The effects of concentration of acidic metal (Al) loading and dehydrating methods (hot air-drying and freeze-drying) were investigated. The BC supported alumina catalysts were characterized by XRD, N_2 physisorption, SEM, FT-IR, back titration, and TGA. After that, the catalytic activity was tested for ethylene production by dehydration reaction of ethanol in gas phase at atmospheric pressure and temperature in the range of 200 ^{o}C to 400 ^{o}C. It was found that Al loading had a significant effect on surface area and acidity of the catalysts. Increase in Al loading resulted in decreased surface area but increased acidity property. In this study, the 50Al/BC-TD catalyst exhibited the highest ethylene selectivity and ethanol conversion at the reaction temperature of 400 ^{o}C.

Department:	Chemical Engineering	Student's Signature .....
Field of Study:	Chemical Engineering	Advisor's Signature .....
Academic Year:	2014	Co-Advisor's Signature .....

ACKNOWLEDGEMENTS

First and foremost, I would like to thank my thesis advisor, Associate Professor Muenduen Phisalaphong, Ph.D. for her invaluable supervisions, creative guidance and encouragement through this thesis work. My appreciation is also extended to my thesis co-advisor, Associate Professor Bunjerd Jongsomjit, Ph.D. on his valuable suggestion and guidance. Without all the support that I have always received from both of them, this work would have never been achieved.

In addition, I am also grateful to convey my appreciation to Associate Professor Artiwan Shotipruk, Ph.D. who has been chairman of the thesis committee. I am also thankful to Associate Professor Joongjai Panpranot, Ph.D. and Narongsak Chaiyasit, Ph.D., as members of the thesis committee for their suggestions and spending time in review my thesis.

Sincere thank is given to Chula Unisearch, Chulalongkorn University for the financial support of this work and special thanks to Begemann Mercury Technology Pacific (BMTP) Co., Ltd. for laboratory supports.

Finally, I most gratefully to my parents and my friends in Biochemical Engineering Research Laboratory and Center of Excellent on Catalysis & Catalytic Reaction Engineering, Chulalongkorn University for all their supports throughout the periods of this research. To others, whose names not specifically mentioned, but have provided me with support and encouragement, please be assured that you will be always remembered and are also a big part of this work.

CONTENTS

Page

Page

Page

Page

LIST OF TABLES

Page

LIST OF FIGURES

Page

LIST OF SCHEMES

Page

CHAPTER I

INTRODUCTION

1.1 Background and rationale

Recent advances in the field of biomaterials and their applications have been gained much interest. Cellulose, a linear biopolymer, is one of the most abundant organic materials with a variety of useful applications. It is found in nature as structural component of the cell wall of plants and algae [1, 2]. However, plant cellulose is unpurified cellulose associated with other kinds of natural fiber like lignin and hemicellulose while bacterial cellulose (BC) is nearly-purified one. Moreover, production of plant cellulose products is facing some environmental problems [3]. Therefore, the production of cellulose by using *Acetobacter xylinum* has been developed [4]. BC can be extracellularly synthesized into nano-sized fibrils by the bacteria *Acetobacter xylinum*, using glucose as a common substrate. Plant-derived cellulose and BC have the same chemical structure. However, BC displayed advantages superior to the counterpart from plants with its physical and chemical properties. It has the unique properties including ultrafine nanofiber network structure, high mechanical strength, high crystallinity and high hydrophilicity.

BC offers a wide range of applications. The oldest use of BC is in the food industry as raw material of nata de coco in the Philippines [5]. BC later has applications in the fabrication of reinforced paper [6]. Recently, BC has become relevant material for medical applications such as temporary skin substitute for patients with extensive burns [7], artificial blood vessels for microsurgery [8], tissue engineering of cartilage [9] and

wound dressing [10]. Due to its good mechanical properties, high water retention capacity, high chemical stability and the ultrafine three-dimension nanofiber network structure endow BC to have extensive specific area, which is advantageous to function as matrix or support for heterogeneous catalysts [11-13]. In this present study, aluminum was loaded into the BC nanofiber and its application was explored for catalysis of ethanol dehydration to ethylene.

Ethylene is one of the most important raw materials in the petrochemical industry. Almost of petrochemical products are produced from ethylene. It can be used as a polymerization raw material to produce a variety of important organic chemical products such as polyethylene, polyvinyl chloride and polystyrene. Moreover, ethylene is also used as the precursor for synthesis of ethylene oxide, ethylene dichloride, ethylene glycol, ethylbenzene, etc. [14-18]. Traditionally, the main process to produce ethylene is hydrocarbon-cracking using petro-hydrocarbon or natural gas as raw material at high temperature [14, 19, 20]. However, with rapid economic growth and industrial production capacity increasing, the demand of nonrenewable fossil fuels also has increased. Therefore, the renewable energy sources have been considered. The dehydration of alcohol has been developed as promising alternative approach to produce ethylene. Dehydration of ethanol over solid acid catalysts requires lower temperature compared to the hydrocarbon-cracking, leading to the energy cost reduction and more environmental friendly. So, different catalysts have been investigated to increase ethylene yield and lower reaction temperature. Besides the reaction temperature, the acidity of the catalysts is one of the most important factors that affected the ability of this reaction.

According to the advantageous properties of BC and important applications of ethylene as an intermediate in the petrochemical industry, this study aims to develop the

bacterial cellulose supported alumina catalysts for ethanol dehydration reaction to ethylene. The catalysts were prepared, characterized, and tested catalytic activity and also the influences of concentration of acidic metal (Al) loading and dehydrating method on dehydration reaction were examined in order to identify suitable BC supported alumina catalysts for ethanol dehydration to ethylene.

1.2 Research objectives

- To develop and characterize alumina catalyst supports derived from bacterial cellulose (BC) of *Acetobacter xylinum*.
- To investigate effects of concentration of acidic metal (Al) loading and dehydrating method on physical and chemical characteristics and catalytic properties of BC supported alumina catalysts for ethanol dehydration to ethylene.
- To identify the optimal conditions for the preparation of BC supported alumina catalyst which gives the highest ethylene selectivity and ethanol conversion.

1.3 Research scopes

- Preparation of bacterial cellulose (BC) supported alumina catalysts by wet impregnation method.
- Investigation effect of concentration of acidic metal (Al) loading on BC, varied from 3 to 14 %w/v of aluminium nitrate aqueous soaking solution.

- Investigation effect of dehydrating methods (hot air-drying and freeze-drying) of BC-Al product after soaking in aluminium nitrate aqueous solution.

- Characterization of the catalysts were undertaken by methods as the following:

  - The catalyst structures and crystallinity were characterized using X-ray diffraction (XRD).

  - The surface area, pore volume and pore size diameter were characterized using N_2 physisorption (BET).

  - The morphology and elemental distribution of the catalysts were characterized using both Scanning Electron Microscopy (SEM) and Energy Dispersive X-ray spectroscopy (EDX), respectively.

  - The total acidity of the catalysts was investigated by acid-base back titration.

  - The functional groups of the catalysts were characterized using Fourier Transforms Infrared spectroscopy (FT-IR).

  - The thermal decomposition of the catalysts was investigated using Thermal Gravimetric analysis (TGA).

- Investigation of catalytic activity of bacterial cellulose supported alumina catalysts in ethanol dehydration under atmospheric pressure and temperature in the range of 200 ^{o}C to 400 ^{o}C.

1.4 Research methodology

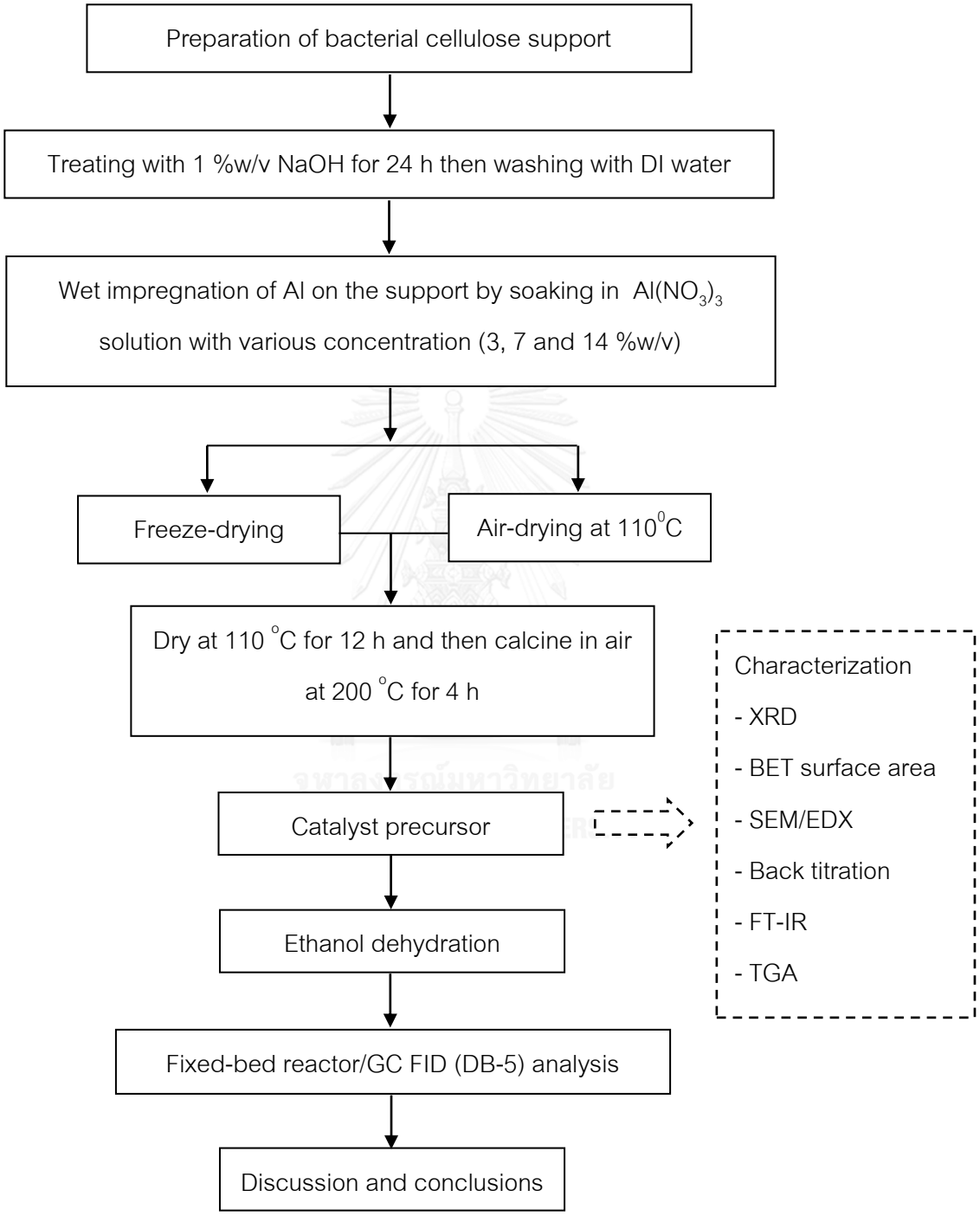

Scheme 1.1 Diagram of research methodology.

CHAPTER II

THEORY

2.1 Cellulose

Cellulose is a biopolymer present in nature as structural component of the cell walls of plants and algae, and it is the most abundant organic compound on Earth. This linear polymer, with molecular formula $(C_6H_{10}O_5)_n$, is composed of repeating β-1, 4-linked D-glucose units [2, 21]. Cellulose molecule forms a straight, almost fully extended chain as shown in **Figure 2.1** [22].

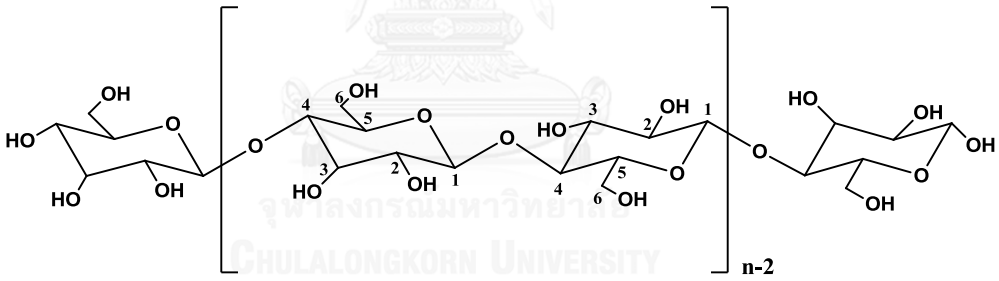

Figure 2.1 Structure of cellulose polymer.

The cellulose chains are organized in a crystalline or semi-crystalline lattice, thus giving rise to microfibrils with a high tensile strength. Cellulose is an insoluble structure. In general, the advantages of cellulose include high specific strength and good thermal stability.

2.2 Bacterial cellulose

Bacterial cellulose (BC) has generally been biosynthesized by *Acetobacter xylinum* [23]. *A. xylinum* is a simple Gram-negative bacterium which has an ability to synthesize a large quantity of high-quality cellulose organized as twisting ribbons of microfibrillar bundles [10]. It can be produced from many different substrates such as Nata de pina and Nata de coco, synthesized by using *A. xylinum* with pineapple water and coconut water as medium, respectively. Morphologically, the reproducible pellicle is obtained by controlling parameters of bacterial growth, for instance, the composition of the culture media, pH, temperature, and oxygen tension.

Glucose is employed as a common substrate. Nonetheless, other simple carbohydrates, alcohols, or polyalcohols can be considered as carbon sources [24]. During the process of actual biosynthesis, many carbon compounds of the nutrition medium are utilized by the bacteria, then polymerized into single, linear β-1, 4-glucan chains and finally secreted outside the cells through a linear row of pores located on their outer membrane. Bacteria build bacterial cellulose (BC) and confine themselves in it to protect themselves from enemies and heavy metal ions while nutrients can be supplied by diffusion [25].

BC traditionally originates as a white gelatinous pellicle on the surface of the liquid medium in a static culture. These bacteria produce cellulose nanofibrils of 3 - 8 nm diameters. Together, the mesh of these fibrils forms a gelatinous membrane. The size of BC fibrils is about 100 times smaller than that of cellulose from plant [10]. This unique nano-structure results in a larger surface area. BC has outstanding tensile strength, high crystallinity, pure fiber network structure, and especially remarkable water holding capacity. It is extremely hydrophilic, absorbed in the range of 60 to 700 times its weight in water [26]. Another advantage of BC over plant cellulose is its higher purity; it does

not contain lignin or other contaminants as its counterpart. Consequently, BC can be easily purified with the use of NaOH with less energy consumption [27].

BC can be synthesized by several producers as shown in **Table 2.1**. The polymer structure depends on the organism. *Acetobacter xylinum* is the best known representative BC producer.

All strains of *Acetobacter xylinum* produce cellulose extracellularly in the form of flat, twisting ribbons. They have been used ordinarily for production of vinegar from wine, and utilized for production of gluconic acid, ketogluconic acids and sorbose as well [4].

Table 2.1 BC producers.

Genus	Cellulose structure
Acetobacter	Extracellular pellicle composed of ribbons
Achromobacter	Fibrils
Aerobacter	Fibrils
Agrobacterium	Short fibrils
Alcaligenes	Fibrils
Pseudomonas	No distinct fibrils
Rhizobium	Short fibrils
Sarcina	Amorphous cellulose
Zoogloea	Not well defined

2.3 Ethanol dehydration

Ethanol to ethylene reaction occurs through ethanol dehydration under the condition of appropriate temperature and the effect of the catalyst. Ethanol catalytic dehydration to ethylene is the earliest used process in the industry [28]. Ethanol

dehydration requires an acid catalyst that has direct influence on the dehydration activity. The common used solid catalysts such as ZSM-5, HZSM-5 zeolite [29, 30], SAPO-34, heteropolyacids [17], and alumina [18, 31] have been applied to investigate the effect of acidity on the ability of ethanol dehydration.

Ethanol, consisting of hydroxyl group in the molecule, can be dehydrated by using acid catalysts. In the catalytic dehydration of ethanol to form ethylene, an acid catalyst first protonates the hydroxyl group, which leaves as a water molecule. The conjugate base of the catalyst then deprotonates the methyl group, and the hydrocarbon rearranges into ethylene [32]. The reaction is endothermic, and because of this, the optimum reaction temperature is in the range of 180 ^{o}C to 500 ^{o}C [33]. The chemical equation of ethanol dehydration reaction is shown in equation (1) and (2) as following [34];

$C_2H_5OH \longrightarrow C_2H_4 + H_2O$ +44.9 kJ/mol (1)

$2C_2H_5OH \longrightarrow C_2H_5OCH_5 + H_2O$ -25.1 kJ/mol (2)

The first equation (1), main reaction, reveals that the reaction of ethanol to ethylene is endothermic reaction while the equation (2), side reaction, shows the reaction of ethanol to diethyl-ether (DEE), which is occurred at low temperature because of its exothermic reaction. Besides, acetaldehyde is byproduct which is formed at high temperature.

The ethanol dehydration reaction has required the acid catalyst consisting of the BrØnsted acid site on surface of catalyst combining with hydroxyl groups. It generates a water molecule, which is emitted [35]. This mechanism of ethanol dehydration to ethylene is shown in **Figure 2.2**. It indicates that ethanol dehydration to ethylene is

elimination reaction type E1. The E1 reaction is divided to 3 steps [15] as described below;

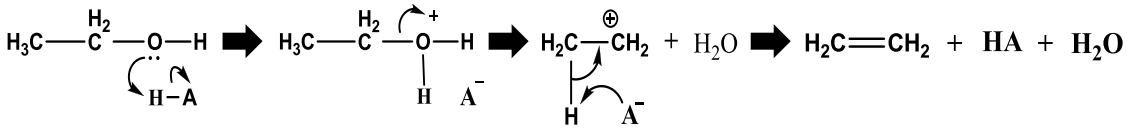

Figure 2.2 Mechanism of ethanol dehydration to ethylene.

Step 1: The hydroxyl group in ethanol molecule is leaving group, when proton from acid catalyst adds into the alcoholic oxygen, it makes a better leaving group. This process is called “protonation”. The long pairs on the oxygen make it a Lewis base. This step is very fast and able to be reversible.

Step 2: Breaking of the C-O bond is endothermic. It causes the loss of the good leaving group (a water molecule) resulting in a carbonation intermediate. This is slow step or the rate determining step.

Step 3: The conjugate base (a water molecule) deprotonates in methyl group leading to the rearrangement of the C=C bond.

In addition, the reaction of the ethanol intermolecular dehydration to diethyl-ether is substitution reaction. The generation of diethyl ether essentially follows the reaction mechanism of single-molecule nucleophilic substitution reaction (S_N1) or bimolecular nucleophilic substitution reaction (S_N2) [36].

The S_N1 reaction is divided into two steps, the first step is that reactants dissociate to carbocations and the negatively charged leaving group, which is the rate-limiting step

and the second step is the carbocations associate with nucleophiles with an extremely fast rate, which is a first-order reaction. For the S_N2 reaction, the lone pair electrons of the nucleophile attack the electrophilic electron deficient central atom, creating the intermediate, and at the same time, removing leaving base-group. In the S_N2 reaction, there is no carbocations created. The S_N1 and S_N2 reaction mechanisms of ethanol dehydration to diethyl-ether are shown as **Figure 2.3** and **Figure 2.4**, respectively [17].

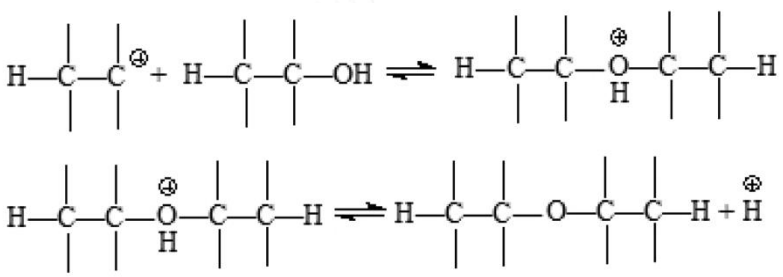

Figure 2.3 The S_N1 reaction mechanism of ethanol dehydration to diethyl-ether.

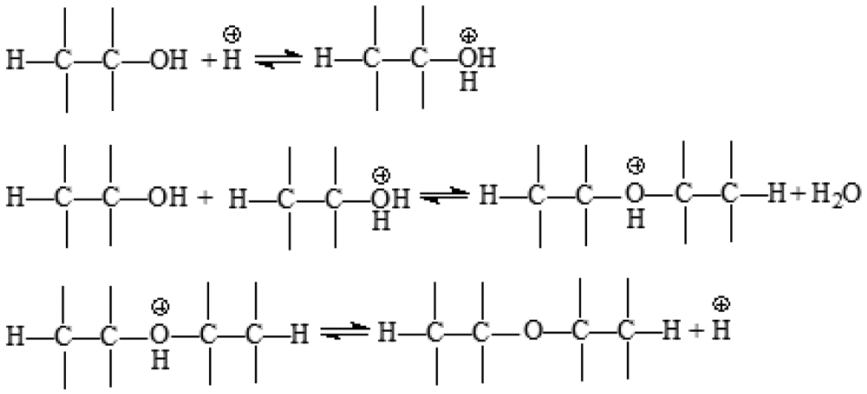

Figure 2.4 The S_N2 reaction mechanism of ethanol dehydration to diethyl-ether.

2.4 Alumina

The catalytic properties of alumina or aluminum oxide have been focused on in an important number of studies and a few articles of synthesis due to the face that aluminum oxide has remarkable adsorbent properties and is capable of activating a certain number of bonds such as hydrogen-hydrogen, carbon-hydrogen, and carbon-carbon bonds. Because of this fact, it features activity in the dehydration of alcohols to ethers or alkenes [37].

The structure of alumina consists of morphology and crystalline structure which has the general form as Al_2O_3. The alumina was discovered as a material existed in natural clay in 1754 by Marggraf [38]. The approximate surface areas are about 100 to 600 m^2/g. These properties depend on the synthesis method, water desorption, impurity and heat treatment. There are many phases of alumina as remarked with Greek alphabet as follows: beta phase, gamma phase, eta phase, chi phase, kappa phase, delta phase, theta phase and alpha phase. Each is unique crystal structure and properties. The phase of alumina depends on calcination temperature of reactant (gibbsite, boehmite, and etc.) [39].

The surface of alumina contains acid and basic sites. The acid site on surface is Lewis and Brønsted acid site which is received from Al^{3+} ion and water molecule coordinated with cation, while the basicity on surface is derived from basic hydroxide group and O^{2-} anion.

The acidity and basicity of alumina is able to be alternated due to the existence or distinction of hydroxyl group from water molecules. The position of acidity is assigned by H_2O molecules coordinated with cationic sites and Al^{3+} ions, while the basicity is defined by O^{2-} anion vacancies and hydroxyl group [40]. When alumina

contacts with humidity, the water molecules have adsorbed on alumina surface and dried in air at temperature between 100 °C to 150 °C, the water molecules are removed, but remain hydroxyl group on alumina surface and generate Lewis acid site and basic site. In case of adding water molecules, Lewis acid site is transformed into Brønsted acid site, which is very weak [41, 42]. The mechanism of alumina acidity is displayed in Figure 2.5.

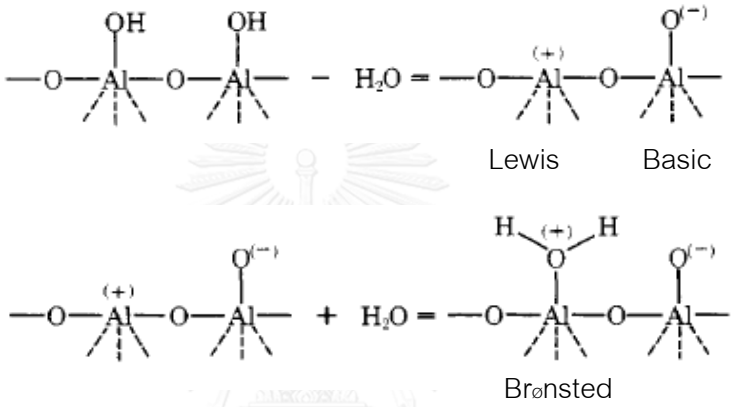

Figure 2.5 Mechanism of alumina acidity.

Alumina has been used as commercial catalyst or support for many industrial processes. The use of alumina in catalyst provides excellent high degree of metal dispersion, moderate high surface area, and thermal stability over wide range of temperature.

CHAPTER III

LETUREATURE REVIEW

3.1 Application of BC

BC offers a variety of useful applications. This is due to the unique properties including high purity with an ultrafine nanofiber network structure, high mechanical strength, and high hydrophilicity. The main potential BC applications are following:

Food applications

The oldest use of BC is in the food industry as raw material of nata de coco in the Philippines [5]. Another popular BC containing food product is Chinese Kombucha or Manchurian Tea, obtained by growing yeast and Acetobacter in a medium containing tea extract and sugar, which might have function to protect against certain cancers. The pellicle was formed on the surface contains both cellulose and enzymes, which are healthy for humans [43]. Moreover, the BC has been applied as a functional food additive to reduce a thickener, texturizer, and/ or calorie (such as ice cream, salad dressing, and weight-reduction base). It was shown that BC from an agitated culture has a much higher emulsifying effect than that from a static culture, because the former has a disordered structure [44].

Paper products

The different application of BC was found to have a remarkably high retention aid function for paper making [6]. BC also was reported as a valuable component for synthetic paper. Since nonpolar polypropylene and polyethylene fibers, providing

insulation, heat resistance, and fire-retarding properties, cannot form hydrogen bonds. The amount of wood pulp in this type of paper is usually from 20 % to 50 % to make high quality papers [43].

Medical applications

Because BC has high tensile strength, durability, and permeability to liquid and gases, it becomes relevant material for medical applications such as temporary skin substitute for patients with extensive burns [7], artificial blood vessels for microsurgery [8], tissue engineering of cartilage [9] and wound dressing [10]. The other commercial application of *A. xylinum* cellulose, like Biofil®, Bioprocess®, and Gengiflex® are realities in the health-care sector. Biofil® displayed to be excellent as skin transplants and treatment of second and third degree burns, ulcers and decubitus while Gengiflex® was successfully applied to recover periodontal tissues [4].

Matrix or support for heterogeneous catalyst

BC has also been used as matrix or support for heterogeneous catalysts due to its great water retention capacity, high chemical stability and the ultrafine three-dimension nanofiber network structure endow BC to create extensive specific area [11-13]. These properties are interesting to explore the applicability of catalyst over the support derived from BC such as BC nanofibers supported palladium catalyst for Heck reaction [45] and biotemplated preparation of CdS nanoparticles/BC hybrid nanofibers for photocatalysis application [46].

3.2 Catalysts in ethanol dehydration reaction

The acidity of catalyst displays important role for the ethanol dehydration reaction to ethylene. Many researchers have investigated to improve and develop the catalyst for many years. The dehydration of ethanol was used phosphoric acid for first study in 1930. Pan (1986) [47] had lather studied phosphate loading on clay and coke supports. In addition, the parameters for ethanol dehydration such as ethanol concentration, reaction temperature, space velocity, and life span of catalyst were studied [48]. The advantages of phosphoric acid catalyst were high ethylene yield. However, the catalysts were rapid deactivated by carbon deposition on catalyst surface.

Acid carbon catalysts had been studied in gas phase ethanol decomposition [14]. The acid nature of solid catalyst has direct influence on the dehydration activity. The acid carbon catalysts were obtained by chemical activation of olive stone with phosphoric acid, without needing additional oxidative treatments. Different impregnation ratios, between 0.5 and 2.0, and activation temperatures, in the range of 400 ^{o}C to 800 ^{o}C, were used for the preparation of the carbons. Impregnation ratio shows more influence in the porous structure development than that observed for the activation temperature. The catalytic decomposition of ethanol over the activated carbons yields mainly dehydration products, mostly ethylene with lower amounts of diethyl ether. In absence of oxygen the catalysts suffer a progressive deactivation. However, the presence of oxygen produces a significant increase of the ethanol conversion without any significant change in the selectivity of reaction and avoids deactivation of the catalysts under the operation conditions studied. The results suggested that oxygen inhibits coke deposition on the acid active sites. Ethanol conversion remains practically constant and selectivity does not change when water vapor is added to the reactor feed in concentration similar to that of bio-ethanol.

Many researchers have reported that HZSM-5 zeolite is also used as a solid catalyst in ethanol dehydration. The acidity and pore of HZSM-5 catalyst are important role for hydrocarbon forming [49]. However, the acidity of the catalyst affects to coke formation on the surface resulted in a decrease in catalytic activity and short life span. Moreover, the acidity of HZSM-5 catalyst for ethanol dehydration can be improved by the addition of metal such as lanthanum, iron, and phosphate [30, 50, 51].

The gamma alumina is used in ethanol dehydration to ethylene. It was found that gamma alumina deactivated slowly compared with clay. However, clay provides ethylene yield higher than that obtained from gamma alumina. Comparing the gamma alumina with HZSM-5 catalyst, gamma alumina provided lower selectivity of ethylene and conversion of ethanol than HZSM-5 catalyst, while the higher reaction temperature than HZSM-5 [30, 34, 50].

Zhang *et al.* (2008) [52] studied gamma alumina used in ethanol dehydration at 475 ^{o}C that gave ethylene selectivity to 90.1%, while the gamma alumina doped with TiO_2 had increased ethylene selectivity to 99.4% at 500 ^{o}C and promoted ethylene yield as reported by Chen *et al.* (2007) [34]. Although, the ethanol dehydration to ethylene using gamma alumina obtained better activity than phosphoric acid catalyst, it required high temperature.

Leandro *et al.* (2011) [53] had prepared alumina catalysts with varying porosity by the combination of the sol-gel method and templating with micelle and emulsion. The effectiveness of macropore insertion was evaluated in the model reaction of ethanol dehydration at 300 ^{o}C. The results clearly show that macroporous alumina with well-designed pore structure allows for a rapid diffusion and consequently improve the reaction kinetics. This work highlights that both porosity and acidity must be considered

in the evaluation of the overall activity of porous catalysts prepared by similar procedures.

3.3 Cellulose supported catalysts

Ying *et al.* (2008) [54] synthesized cellulose supported palladium complex to study effect of amount of catalyst on catalytic property by using Heck arylation of acrylic acid with iodobenzene at 90 ^{o}C. The results obtained the reaction can be carried out efficiently with small amount of the catalyst (0.025 mol% Pd), and the yield of the cinnamic acid was 68%. Increasing the amount of the catalyst, the yield of the product enhanced and the reaction time decreased. Nevertheless, the yield of the product and the reaction time changed slightly after the amount of the catalyst was increased to 0.125 mol% Pd. In addition, Peipei *et al.* (2012) [45] reported preparation of BC nanofibers supported Pd catalyst by facile hydrothermal reduction. The Pd/BC catalyst was characterized using various techniques. The results indicated that PdNPs were deposited onto BC nanofibers by physical coating, where the crystalline structures of both Pd and BC remained unchanged after deposition of PdNPs. The catalysis results showed Pd/BC catalyst was a highly efficient and recyclable catalyst for standard Heck coupling reaction. The robust catalyst can be recycled as least 5 times with the coupling yields maintaining 90%.

Jamwal *et al.* (2011) [55] reported simple preparation of Pd(0) nanoparticles dispersed on the surface of cellulose for the Suzuki coupling between aryl bromides and phenyl boronic acid in water, and aerobic oxidation of benzyl alcohols in acetonitrile using air as molecular oxygen source. The Cell-Pd(0) was found to be highly active and could be recycled for 5 consecutive runs. Moreover, Sajjad *et al.* (2013) [56] had also

prepared Pd(0) nanoparticles supported on ethylenediamine-functionalized cellulose catalyst, PdNPs@EDACs, by uniform distribution of PdNPs (average particles size 4.6 to 6.8 nm) onto ethylenediamine-functionalized cellulose. This catalyst was found to be a highly efficient heterogeneous catalyst for the Heck and Sonogashira couplings in water media at 100 ^{o}C in very low loading of Pd. Entrance of ethylenediamine in cellulose structure had advantages such as contribute to a more uniform distribution of palladium on the catalyst surface as indicated by TEM, and improvement of thermal stability in comparison with cellulose as indicated by TGA. Also, the catalyst was showed good chemical stability in the reaction media proved by recyclability of the catalyst at least 4 cycles without losing of its activity.

Heeyeon *et al.* (2012) [57] synthesized porous carbon from natural cellulose fibers and investigated its performance as a catalytic support for a reforming of CH_4 from CO_2. Ni particles supported on cellulose fibers showed little agglomeration, even after a 168 h reforming reaction, but superior catalytic activity and long-term durability compared to a Ni/Al_2O_3 model catalyst. One of the reasons for these results was the lower extent of coking originating from the carbonaceous support. Another reason was the high dispersion of Ni particles on the cellulose support, which was caused by the presence of alkaline earth metals such as Ca and Mg in the original structure of the support.

Inspired by the great success of micro/nanocrystalline cellulose as robust support for heterogeneous catalysts that provide excellent properties, especially in metal dispersion, chemical stability, thermal stability, and recyclability and recent research interest in developing BC nanofibers based functional materials, it is intriguing to explore the applicability of BC supported catalyst in various reactions to respond to the current appeal for ecofriendly and sustainable green chemistry.

CHAPTER IV

EXPERIMENTAL

This chapter explains the laboratory procedures including the catalyst preparation of BC supported alumina catalyst presented in section 4.1, the characterization of catalyst are presented in section 4.2, and the experiment procedure for ethanol dehydration reaction presented in section 4.3, respectively.

4.1 Catalyst preparation

4.1.1 Chemicals

The list of chemicals used in the preparation of catalysts is shown in **Table 4.1**.

Table 4.1 The chemicals used in the catalysts preparation.

Chemical	Supplier
Bacterial cellulose (BC)	Kasetsart University
Sodium hydroxide [NaOH]	Ajax
Aluminium nitrate nonahydrate $[Al(NO_3)_3 \cdot 9H_2O]$	Merck

4.1.2 BC preparation

Bacterial cellulose (BC) was formed by *A. xylinus* (AGR 60) cultures on the surface of a medium containing 0.5% ammonium sulfate, 5.0% sucrose, and 1.0% acetic acid in coconut water. The sheets of BC were purified by washing with deionized

(DI) water, then were treated with 1 wt % NaOH at 35°C for 24 h to remove bacterial cells, and were rinsed with DI water until the pH was 7 [58].

4.1.3 Preparation of BC supported alumina catalysts

The BC samples were first purified by washing with DI water for 1 h and then were treated with 1 %w/v NaOH at room temperature for 24 h to remove bacterial cells followed by rinsing with DI water until pH came to 7.

A 200 g of the purified wet BC hydrogel was soaked in 200 ml of aluminium nitrate aqueous solution with various concentrations (3, 7, and 14 % w/v) for giving 12, 25 and 50 %wt of Al loaded on dried BC after dehydrating. The BC suspensions were stirred continuously overnight at room temperature to obtain equal distribution of Al inside and outside of the BC matrix. Afterward, the obtained BC-Al product was separated to 2 parts. The first one was dehydrated by hot air-drying at 110 ^{o}C for 24 h and calcined in air at 200 ^{o}C for 4 h. The another one was freeze-dried, followed by dehydrating at temperature of 110 ^{o}C for 12 h and calcined in air at 200 ^{o}C for 4 h. The catalysts obtained were stored in plastic film at room temperature.

4.1.4 The nomenclature of catalyst samples

In this research, the nomenclature of a sample is given as follows:

- **xAl/BC-TD** refers to BC supported alumina catalyst dehydrated by hot air- drying after soaking in aluminium nitrate aqueous solution.
- **xAl/BC-FD** refers to BC supported alumina catalyst dehydrated by freeze-drying after soaking in aluminium nitrate aqueous solution.

Where **x** is the wt% of Al loading based on dry weight of BC.

For the example, 50Al/BC-TD means BC supported alumina catalyst with 50 %wt of Al loading based on dry weight of BC after dehydrating by temperature-drying.

4.2 Catalyst characterization

The catalyst was characterized by a variety of techniques as shown below.

4.2.1 X-ray diffraction (XRD)

The bulk phase and X-ray diffraction (XRD) patterns of the catalysts were determined by the SIEMENS D5000 X-ray diffractometer connected with a personal computer with Diffract ZT version 3.3 programs for fully control of the XRD analyzer. The characterization was carried out by using CuK_{α} radiation with Ni filter in the 2θ range of 10 to 80 degree with a resolution of 0.04°.

4.2.2 Nitrogen physisorption

The BET surface area, pore volume and pore diameter of catalysts were measured by nitrogen adsorption-desorption isotherm at liquid nitrogen temperature (-196 $^{\circ}$C) using MicromeriticsChemisorb 2750 Pulse chemisorption system instrument. The surface area and pore distribution were calculated by to Brunauer-Emmett-Teller (BET) and BJH methods, respectively.

4.2.3 Scanning electron Microscopy (SEM) and energy dispersive X-Ray spectroscopy (EDX)

Scanning electron microscopy (SEM) and Energy dispersive X-Ray spectroscopy (EDX) was used to determine the surface morphology and elemental distribution of the catalyst particles. Model of SEM: JEOL mode JSM-5800LV and EDX was performed using Link Isis Series 300 program at the Scienctific and Technological Research Equipment Center, Chulalongkorn University (STREC). Before the determination, the

samples were sputtered with platinum and photographed. The coated specimens were kept in dry place before examination.

4.2.4 Back titration

The total acidity of the catalysts was determined using standard acid-base back titration. Typically, approximately 0.1 g of catalyst sample was put in an Erlenmeyer flask containing 60 ml of 0.008 M NaOH, and stirred at room temperature for 1 h. Then the excessive amount of NaOH was neutralized using 0.02 M HCl as the titrant.

4.2.5 Fourier transform infrared spectroscopy (FT-IR)

FT-IR spectroscopy was used primarily to determine the functional group of the catalyst sample. The Nicolet 6700 FTIR spectrometer was used in this research.

4.2.6 Thermal gravimetric analysis and differential thermal analysis (TGA/DTA)

Thermal gravimetric analysis (TGA) and differential thermal analysis (DTA) were performed using an SDT analyzer Model Q600 from TA Instrument, USA. The TGA/ DTA analyses the catalysts were carried out from room temperature to 800 ^{o}C in air at a heating rate of 10 ^{o}C/min.

4.3 Reaction study in ethanol dehydration

In this proposed research, the ethanol dehydration reaction was tested in gas phase at atmospheric pressure. The reaction was investigated for all catalysts using the apparatus as shown in **Scheme 4.1**.

4.3.1 Chemicals and reagents

The details of chemicals and reagents, used in the ethanol dehydration reaction are shown in **Table 4.2**.

Table 4.2 The chemicals and reagents used in the reaction.

Chemicals and Reagents	Supplier
High purity grade hydrogen (99.99%)	TIG
Ultra high purity nitrogen gas (99.99%)	TIG
Argon	TIG
Ethanol	Merck

4.3.2 Instruments and apparatus

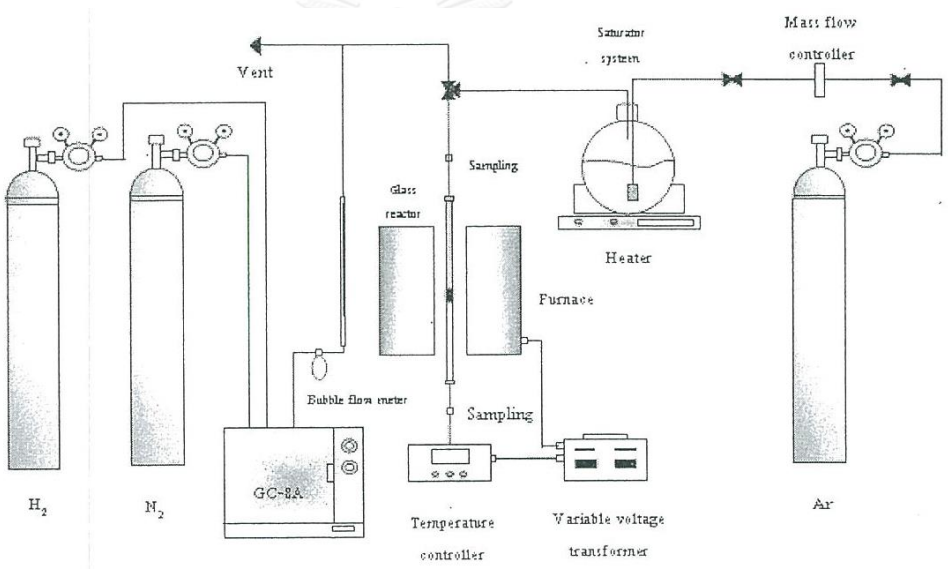

Scheme 4.1 Flow diagram of ethanol dehydration system.

The system of the ethanol dehydration is shown in **Scheme 4.1**. The main instruments and apparatus in the reaction study are explained as follows:

(a) Reactor: The reactor tube is made from glass tube (borosilicate type) with an inner diameter 0.7 mm.

(b) Saturator: The saturator is made from glass. The role of the saturator is to produce ethanol saturated vapor from liquid which is set to bubble ethanol by feeding argon gas and providing heat by a hot-plate. The saturator is operating at atmospheric pressure.

(c) Furnace and heating cable: The furnace is provided heat for the reactor. The temperature of the furnace is controlled by interoperability of variable voltage transformer and temperature controller. For heating cable, it is wrapped with the line at outlet of reactor. The heating cable is used to prevent the condensation of water dehydrated from reaction.

(d) Temperature controller: The temperature of furnace is established a set point at any temperature in the range between 200 ^{o}C to 400 ^{o}C by temperature controller which is connected to thermocouple attached to the reactor and a variable voltage transformer.

(e) Gas controlling system: Argon is used as ethanol vapor carrier into the system. It is set with a pressure regulator, an on-off valve and mass flow controller are used to adjust the flow rate of carrier gas.

(f) Gas chromatography (GC): A gas chromatography (Shimadzu GC-14A) equipped with flame ionization detector (FID) with DB-5 capillary column, which is used to analyze the feed and product. The operating condition for gas chromatography is reported;

- Detector: FID
- Capillary column: DB-5
- Carrier gas: Nitrogen (99.99 vol.%) and Hydrogen (99.99 vol.%)
- Column temperature:

- Initial: 40 °C
- Final: 40 °C

- Injector temperature: 150 °C
- Detector temperature: 150 °C
- Time analysis: 12 min.

4.3.3 Ethanol dehydration reaction procedure

The ethanol dehydration was carried out in a fix-bed continuous flow reactor with an inner diameter 0.7 mm. In the experiment, 0.01 g of a packed quartz wool and about 0.05 g of catalyst were packed in the reactor, and the catalyst was then pretreated in argon (50 ml/min) at 200 °C for 1 h under atmospheric pressure. The reaction was carried out in temperature range of 200 °C to 400 °C. The effluent products were collected and analyzed by a Shimadzu GC8A gas chromatograph with FID using capillary column (DB-5) at 150 °C.

CHAPTER V

RESULT AND DISCUSSION

This chapter describes the results and discussions on the influence of concentration of acidic metal loading and dehydrating method, including hot air-drying and freeze-drying, of bacterial cellulose (BC) supported alumina catalysts. All catalysts were characterized and tested in ethanol dehydration reaction to consider the suitable catalyst and condition for ethanol dehydration to ethylene.

In this chapter, it is divided into two sections: Section 5.1 Characteristic of BC supported alumina catalysts with various concentrations of Al loading and different dehydrating methods and 5.2 Comparison of catalytic activity among BC supported alumina catalysts for ethanol dehydration.

5.1. Characteristic of BC supported alumina catalysts with various concentrations of Al loading and different dehydrating conditions

This section exhibited the characteristic of BC and BC supported alumina catalysts from various techniques including X-Ray Diffraction (XRD), BET surface area, Scanning Electron Microscopy (SEM) and Energy Dispersive X-Ray Spectroscopy (EDX), Fourier Transforms Infrared Spectroscopy (FT-IR), total acidity, and Thermal Gravimetric Analysis (TGA).

5.1.1. X-ray diffraction (XRD)

X-ray diffraction technique was used to identify the bulk structure of catalysts. **Figure 5.1** shows XRD patterns of BC and BC supported alumina catalysts prepared by various concentrations of Al loading and different dehydrating methods.

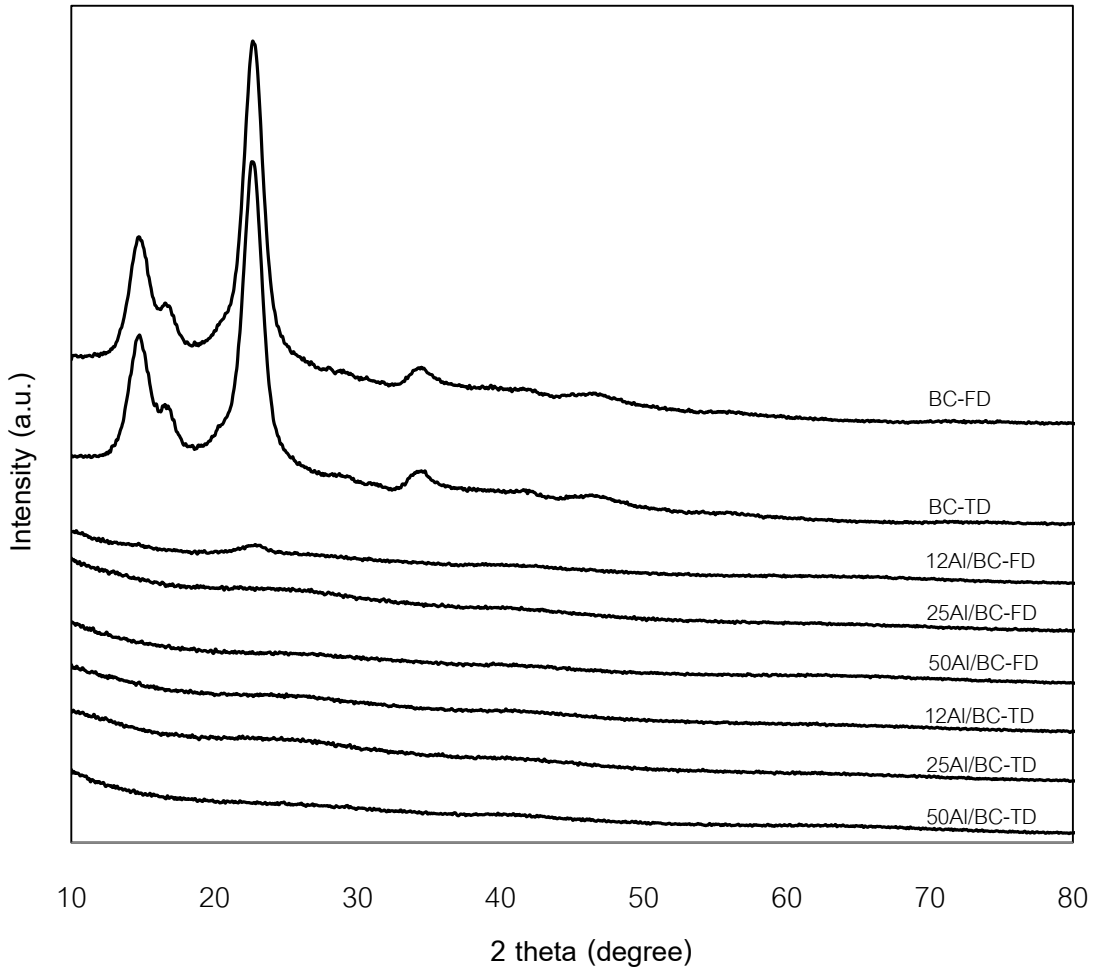

Figure 5.1 XRD patterns of BC and BC supported alumina catalysts.

The XRD pattern of BC, raw material of the catalysts, demonstrated that the peaks observed at 14.4°, 16.6° and 22.4° were attributed to the BC cultured in static circumstance [58]. All BC supported alumina catalysts, both of dehydrating by hot air-drying and freeze-drying showed only a broad diffraction peak around 2θ = 22.5, which

could be described as amorphous carbon composing of aromatic carbon sheets [59]. There were no regular sharp peaks in the XRD patterns of all Al/BC samples; the percentage of crystallinity was close to zero. These results indicated that the highly crystalline structure of unsoaked BC might be totally disrupted after being soaked in aluminium nitrate solution and/or the left over carbons from the calcination might be completely covered by amorphous Al coatings. In addition, based on XRD analysis, all BC supported alumina catalyst samples appeared to be fully amorphous, which should be because they were calcined at quite low temperature (the calcination temperature was 200 ^{o}C).

5.1.2. Nitrogen physisorption

BET surface area, pore volume, and pore size diameter of BC and BC supported alumina catalysts with various Al loading, dehydrated by hot air-drying and freeze-drying are summarized in **Table 5.1**.

Table 5.1 BET surface area, pore volume, and average pore diameter of the BC and BC supported alumina catalysts.

Catalyst Sample	BET surface area S_{BET} (m^2/g)	Total pore volume V_{total} (cm^3/g)	Average pore diameter D_p (nm)
BC-TD	19.210	0.04281	8.9170
12Al/BC-TD	10.470	0.04626	17.6700
25Al/BC-TD	17.670	0.11290	25.5700
50Al/BC-TD	10.500	0.08668	33.0100
BC-FD	63.820	0.27080	16.9700
12Al/BC-FD	20.070	0.13960	20.6200
25Al/BC-FD	21.920	0.14390	26.2600
50Al/BC-FD	15.960	0.13670	34.2500

From **Table 5.1**, it reveals that the BET surface area decreased with an increasing Al loading. The surface area decreased from 19.210 to 10.500 m^2/g and from 63.820 to 15.960 m^2/g with increasing amount of Al loading from 0 to 50 %wt on BC supported alumina catalysts dehydrated by hot air-drying and freeze-drying, respectively. BC supported alumina catalysts dehydrated by hot air-drying method had less surface area than those of freeze-drying method. However, the comparable pore diameters were observed from Al/BC catalysts prepared by both drying methods with the same amount of Al loading. All BC supported alumina catalysts had average pore diameter larger than that of BC. The average pore diameter was increased with an increase of Al loading, which was in the order: 50Al/BC-TD > 25Al/BC-TD > 12Al/BC-TD > BC-TD, for the catalysts dehydrated by hot air-drying and 50Al/BC-FD > 25Al/BC-FD > 12Al/BC-FD > BC-FD, for the catalysts dehydrated by freeze-drying. It was suggested that partial hydrolysis of BC might occur during the processes of soaking in the acid solution and

calcination, resulting in larger pore diameters. The breaking of small pores and combination of small pores into larger pores were previously observed in these kinds of steps [60]. It was denoted that all BC and BC supported alumina catalysts dehydrated by hot air-drying and freeze-drying had mesoporous structures with the average pore diameter in the range of 8 to 33 nm and 16 to 34 nm, respectively.

The type of pores present in the BC and BC supported alumina catalysts can also be confirmed by isotherm curve analysis. The N_2 adsorption-desorption isotherms of the BC and BC supported catalysts with various concentrations of Al loading, dehydrated by hot air-drying and freeze-drying are shown in **Figure 5.2** and **5.3**, respectively. According to IUPAC (International Union of Pure and Applied Chemistry) classification of physisorption isotherms, the isotherms of all BC supported alumina catalysts apparently correspond to type IV isotherms which appear as hysteresis loop at high relative pressure. It reveals that all catalysts display mesoporous structure (pore diameter between 2 and 50 nm). It was shown that Al loading and dehydrating method could affect porous structure in term of surface area, pore volume and pore diameter; however, all BC and BC supported alumina catalysts still had mesoporous structures.

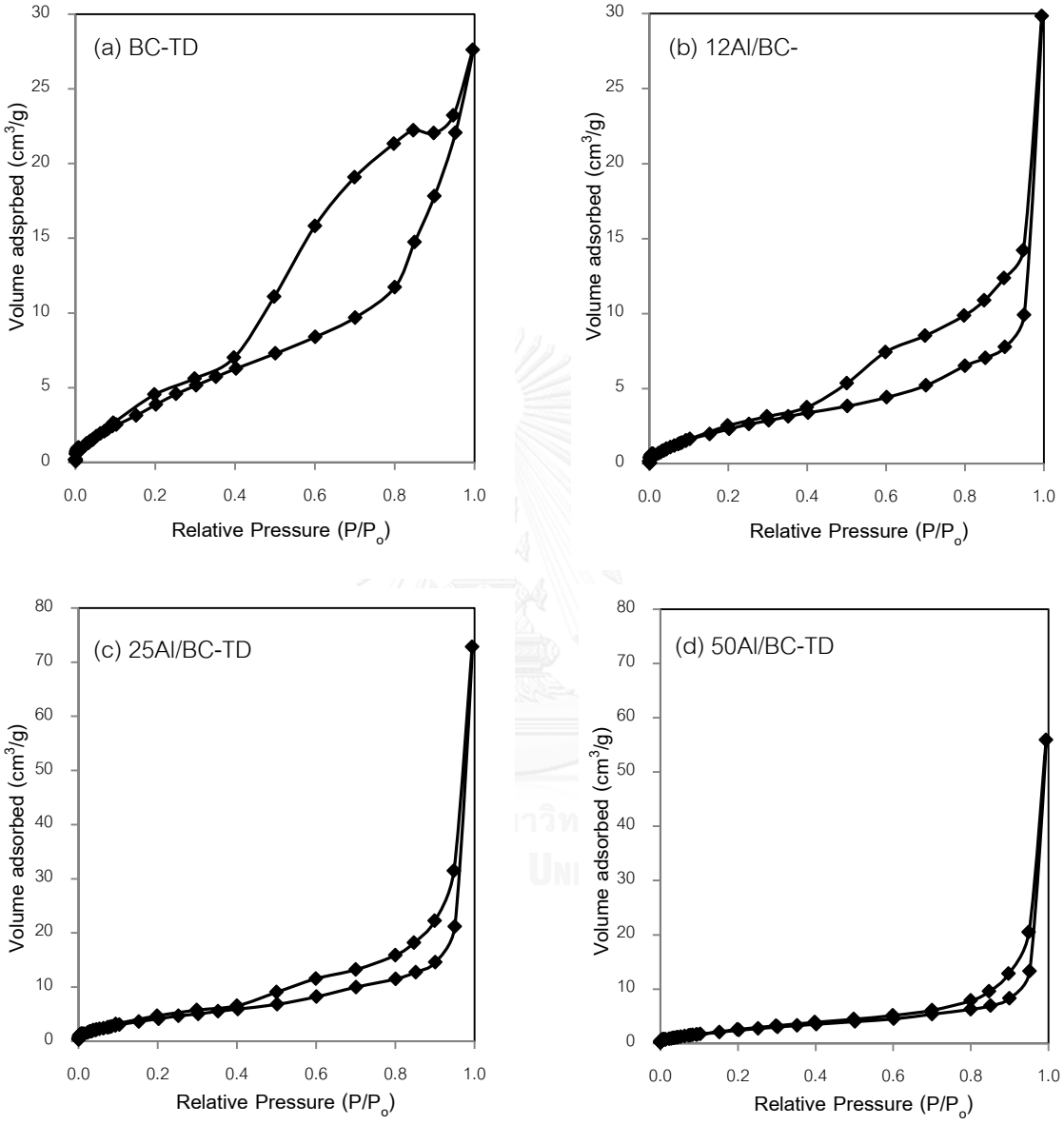

Figure 5.2 The N_2 adsorption-desorption isotherms of BC and BC supported alumina catalysts dehydrated by hot air-drying.

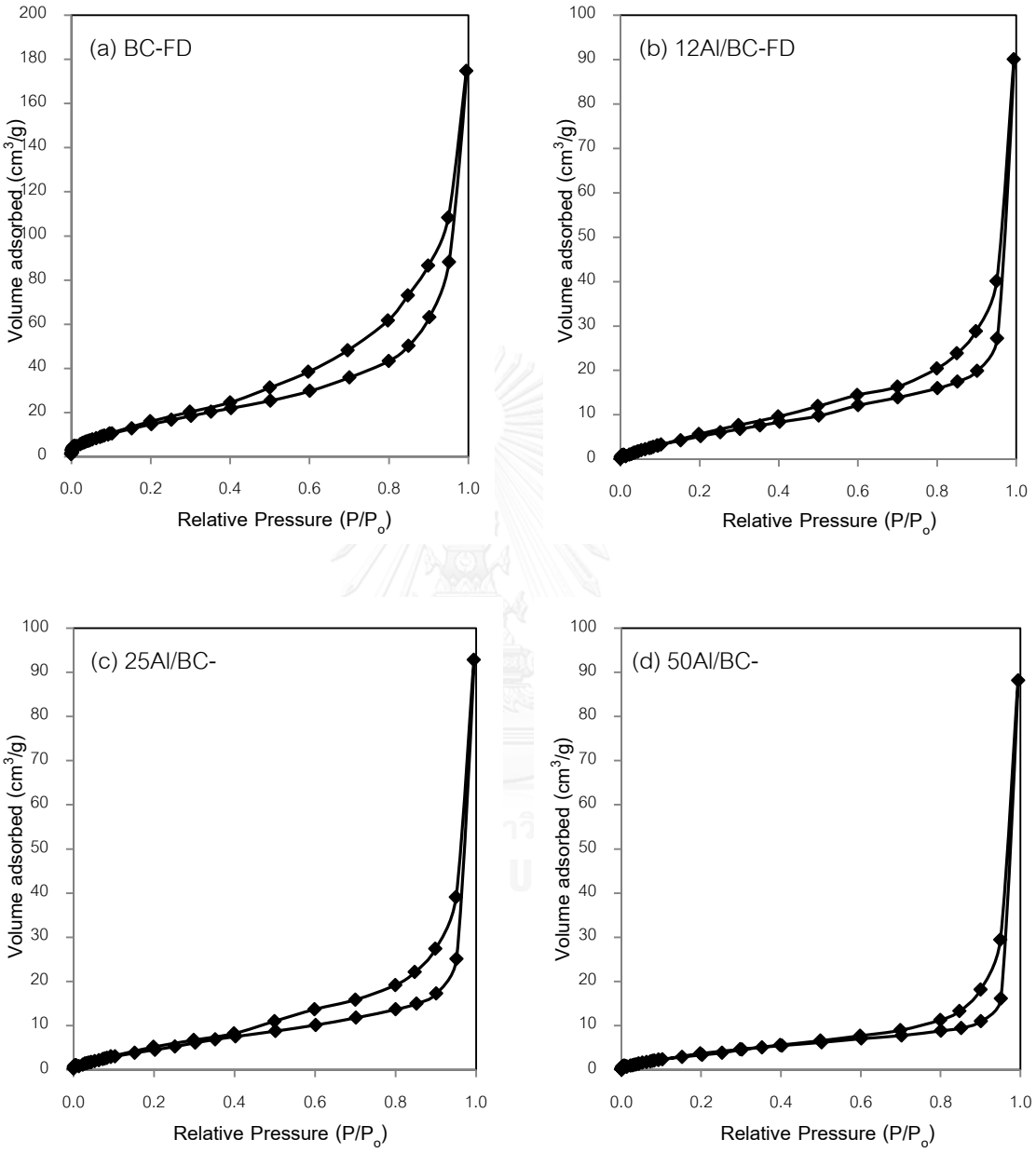

Figure 5.3 The N_2 adsorption-desorption isotherms of BC and BC supported alumina catalysts dehydrated by freeze-drying.

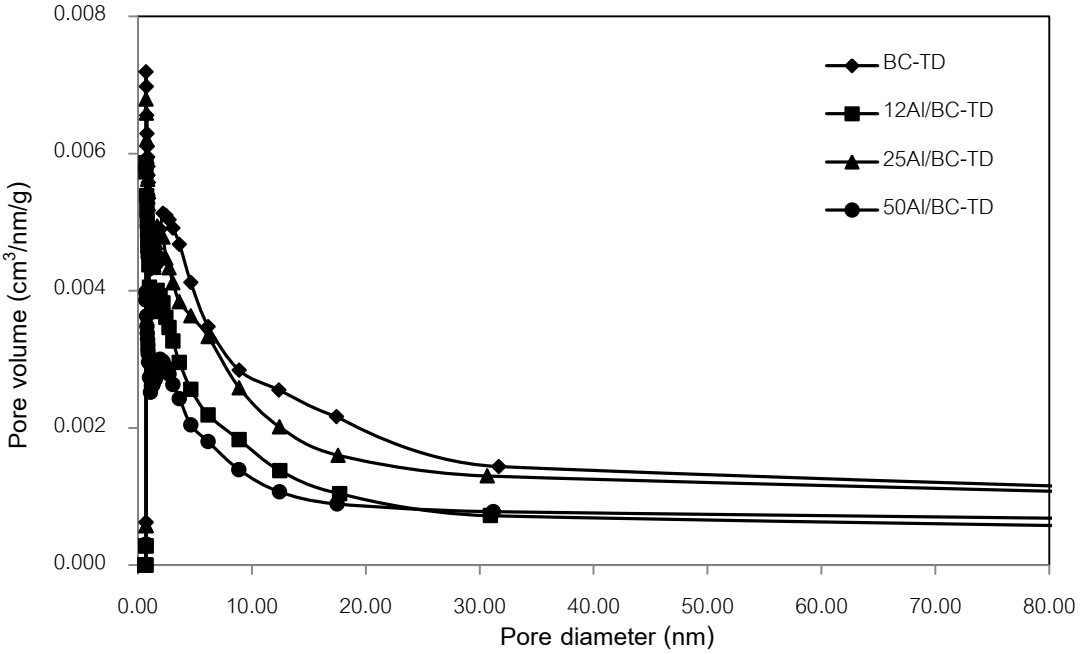

Figure 5.4 BJH pore size distribution of BC and BC supported alumina catalysts dehydrated by hot air-drying.

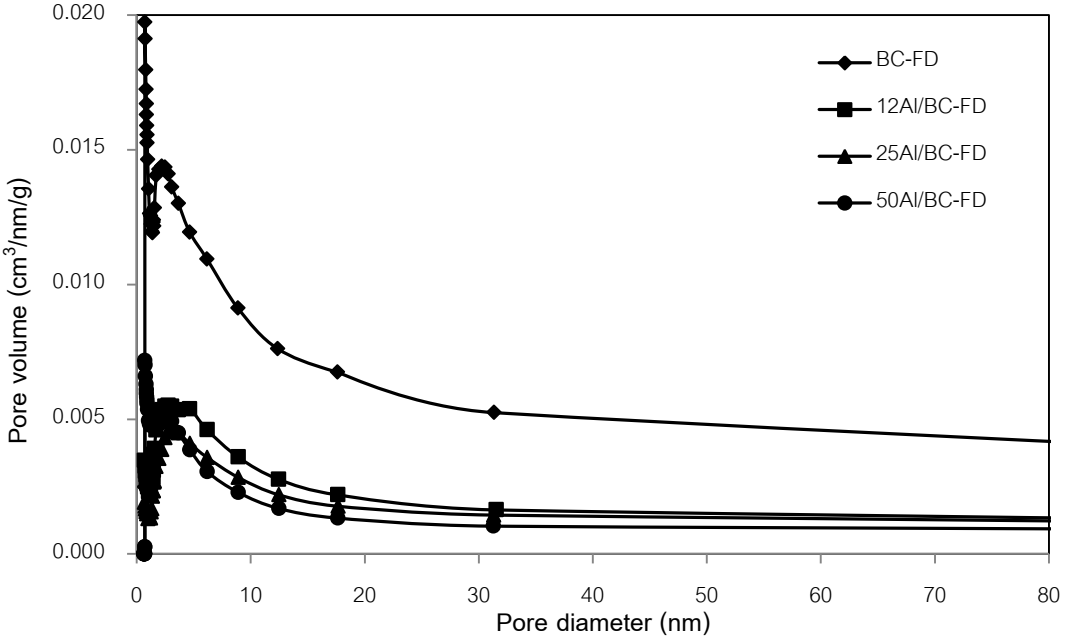

Figure 5.5 BJH pore size distribution of BC and BC supported alumina catalysts dehydrated by freeze-drying.

Pore size distributions of BC and BC supported alumina catalysts, dehydrated by hot air-drying and freeze-drying are shown in **Figure 5.4** and **5.5**, respectively. It is seen that pore size of catalysts is mainly in the range of 2 to 30 nm, which indicates mesoporous type. However, Al/BC catalysts also consisted of the large mesopores of diameter sizes greater than 30 nm.

5.1.3. Scanning electron microscopy (SEM) and energy dispersive X-Ray spectroscopy (EDX)

Scanning electron microscopy (SEM) and energy dispersive X-Ray spectroscopy (EDX) were conducted in order to study the surface morphology and elemental distribution of the samples, respectively.

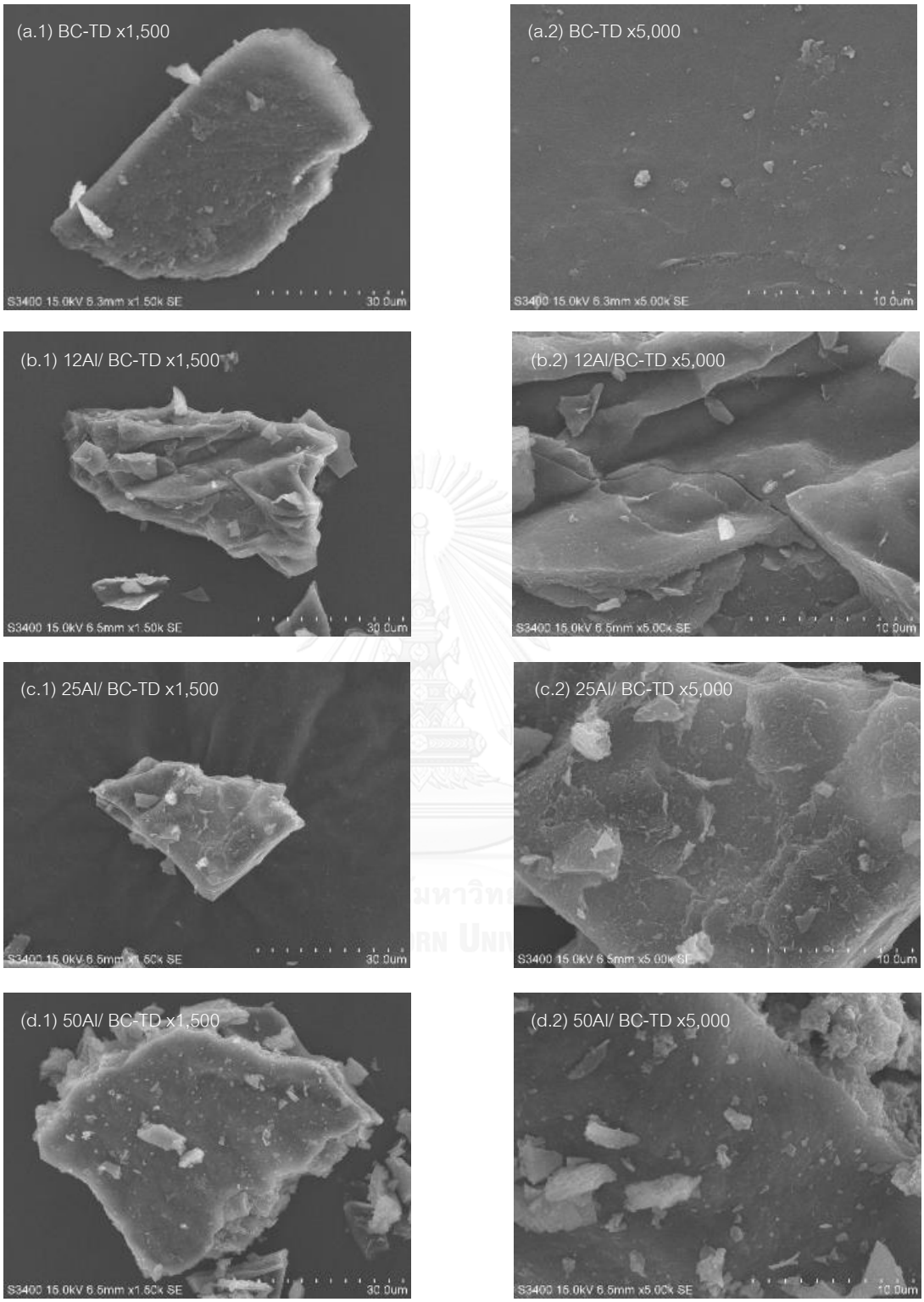

Figure 5.6 SEM micrograph of surface morphology of BC and BC supported alumina catalysts dehydrated by hot air-drying.

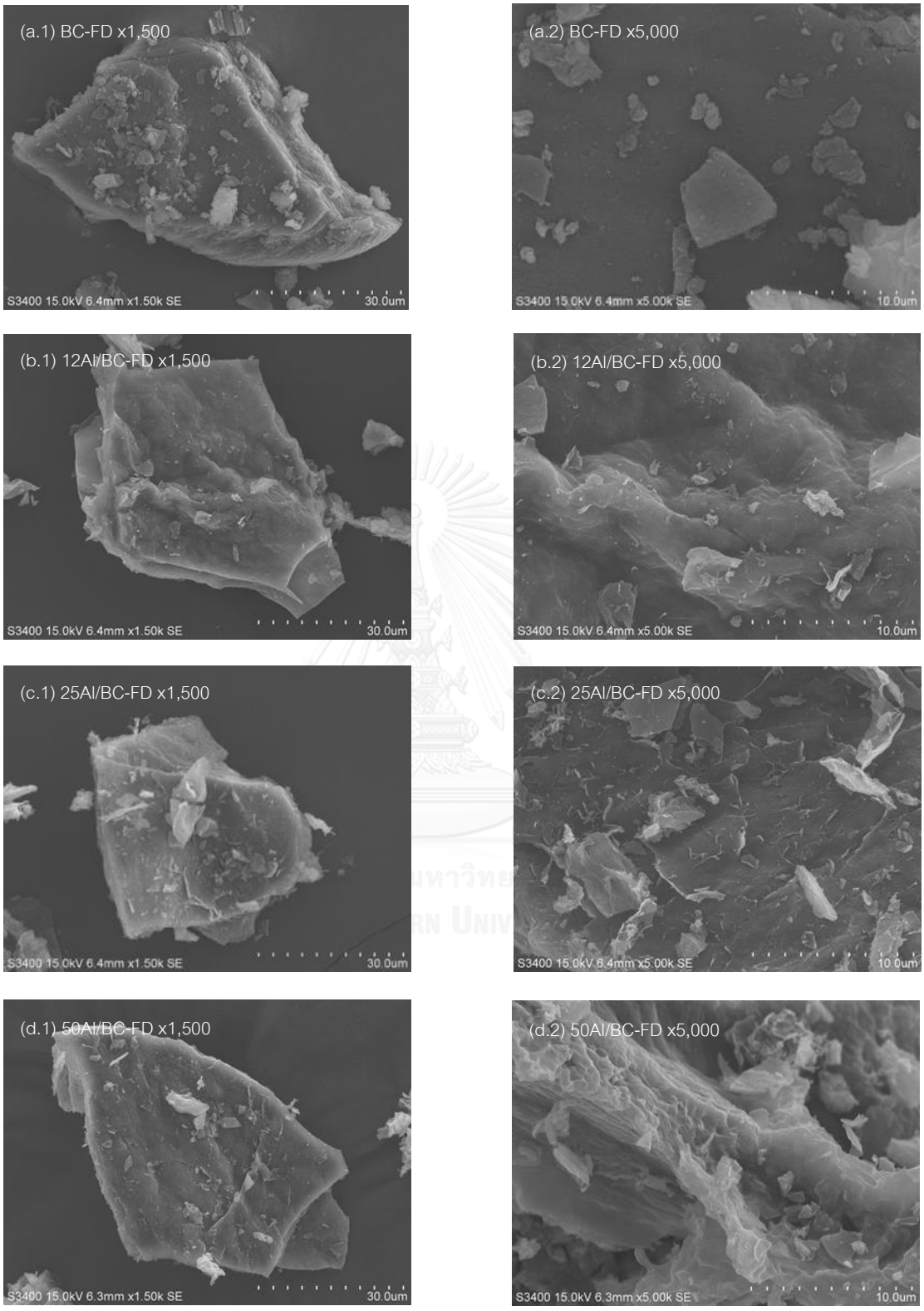

Figure 5.7 SEM micrograph of surface morphology of BC and BC supported alumina catalysts dehydrated by freeze-drying.

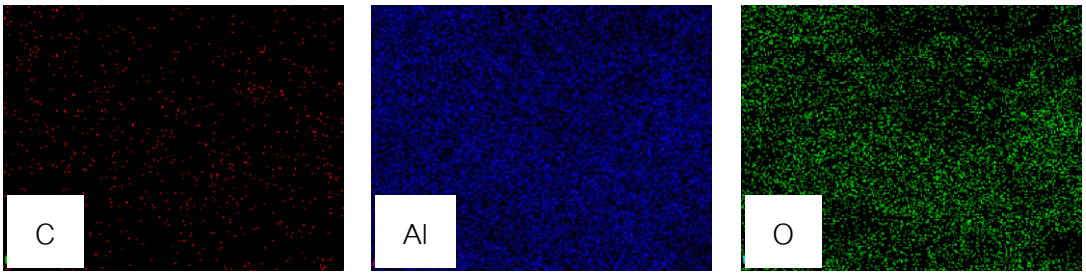

(a) 12Al/BC-TD

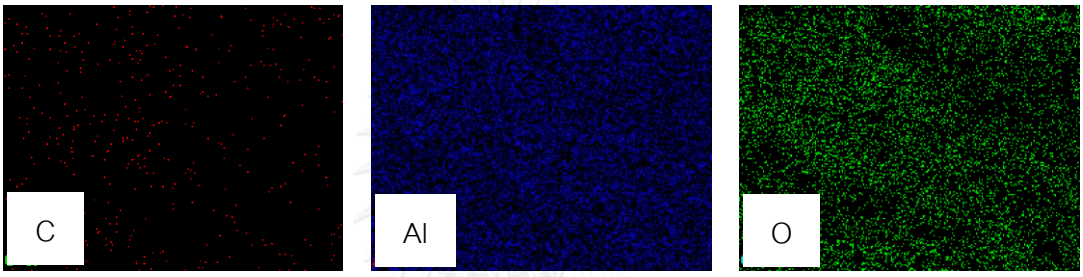

(b) 25Al/BC-TD

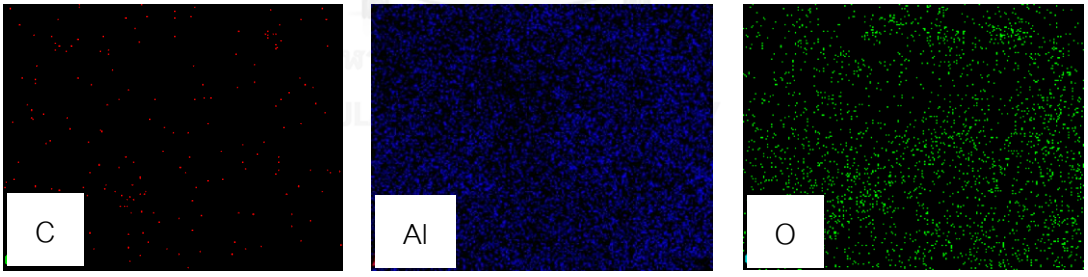

(c) 50Al/BC-TD

Figure 5.8 EDX mapping of BC supported alumina catalysts dehydrated by hot air-drying.

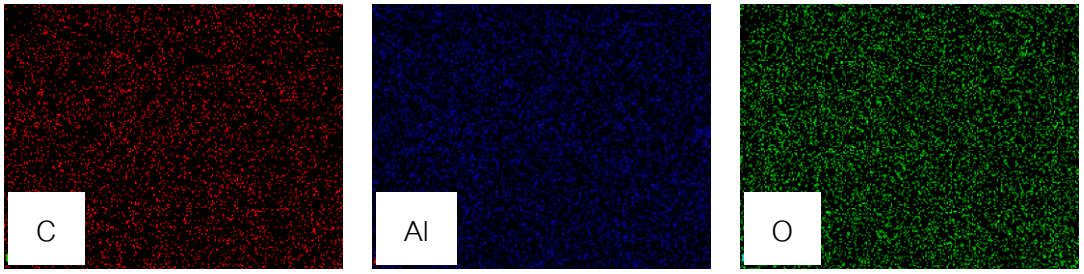

(a) 12Al/BC-FD

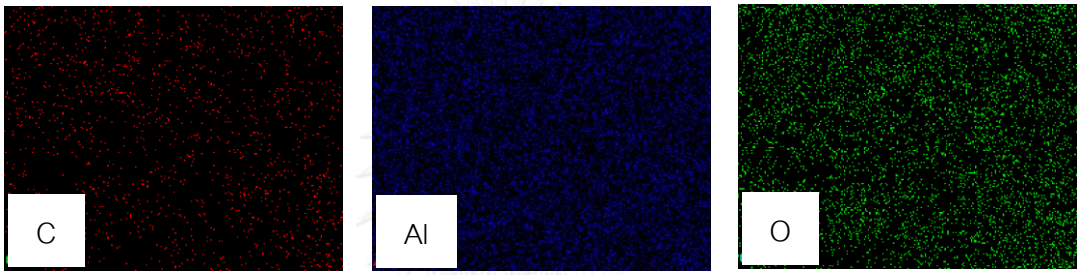

(b) 25Al/BC-FD

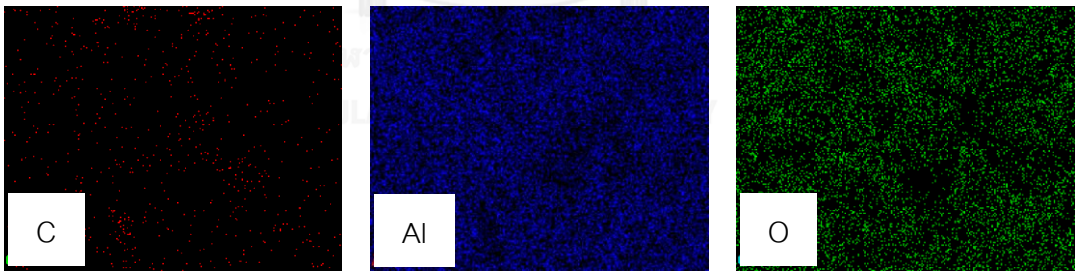

(c) 50Al/BC-FD

Figure 5.9 EDX mapping of BC supported alumina catalysts dehydrated by freeze-drying

Table 5.2 EDX analysis of BC supported alumina catalysts.

Catalyst	% Weight			% Atom		
Sample	C	Al	O	C	Al	O
12Al/BC-TD	8.80	50.42	40.78	14.23	36.28	49.49
25Al/BC-TD	5.46	50.46	44.08	8.94	36.82	54.24
50Al/BC-TD	6.15	60.35	33.50	10.57	46.19	43.24
12Al/BC-FD	31.48	19.49	49.03	40.90	11.27	47.82
25Al/BC-FD	23.94	36.19	39.87	34.21	23.02	42.77
50Al/BC-FD	7.95	55.65	36.40	13.24	41.25	45.50

SEM images in **Figure 5.6** and **5.7** illustrate surface morphology of BC and BC supported alumina catalysts with 12, 25 and 50 %wt Al loading of both dehydrating by hot air-drying and freeze-drying, respectively. Rough surface with clusters of catalyst particles on BC support was observed on Al/BC. The surface of catalyst samples were covered with an amount of alumina as shown in **Figure 5.6(b) – 5.6(d)** and **Figure 5.7(b) – 5.7(d)**. However, from the SEM images, Al- particles and C- particles could hardly be differentiated. Therefore, EDX analysis was used to indicate elemental distribution and to estimate its percentage on surface area of the support. EDX mapping of BC supported alumina catalysts of both dehydrated by hot air drying and freeze-drying is shown in **Figure 5.8** and **5.9**, respectively. It was shown that all of BC supported alumina catalysts exhibited well dispersion of Al on the BC support.

Energy dispersive X-ray spectroscopy (EDX) was performed in order to investigate elemental distribution in the bulk catalyst as shown in **Table 5.2**. It was found that % weight of Al on BC supported alumina catalysts dehydrated by freeze-drying increased by adding of Al, which was 19.49, 36.19 and 55.65 %wt on the catalysts,

12Al/BC-FD, 25Al/BC-FD, and 50Al/BC-FD, respectively. When considered upon the same %loading of Al onto different catalyst, the catalysts dehydrated by hot air-drying presented higher %weight of Al than the catalysts dehydrated by freeze-drying, which is related to the lower of %weight of carbon. As the porous structure of the Al/BC catalysts dehydrated by hot air-drying tended to shrink during drying, the shrinkage in carbon structure could lead to a dense structure, resulting in higher percentage of alumina on the surface.

5.1.4. Total acidity

Standard acid-base back titration can be used to examine total acidity of the catalysts as shown in **Table 5.3**. The total acidity of BC supported alumina catalysts was in the order: 50Al/BC-TD > 25Al/BC-TD > 12Al/BC-TD, for the catalysts dehydrated by hot air-drying and 50Al/BC-FD > 25Al/BC-FD > 12Al/BC-FD, for the catalysts dehydrated by freeze-drying. It obtained that 50Al/BC-TD displayed the highest total acidity which was 2.158 mmol/g.cat. Overall, BC supported alumina catalysts dehydrated by hot air-drying method had higher total acid density than those of freeze-drying method, considering at the same concentrations of Al loading.

Table 5.3 Total acidity of BC supported alumina catalysts.

Catalyst Sample	Total acidity (mmol/g.cat)	Total acid density ($mmol/m^2$)
12Al/BC-TD	1.556	0.1486
25Al/BC-TD	1.621	0.0917
50Al/BC-TD	2.158	0.2055
12Al/BC-FD	0.848	0.0423
25Al/BC-FD	1.417	0.0646
50Al/BC-FD	1.825	0.1143

5.1.5. Fourier transforms infrared spectroscopy (FT-IR)

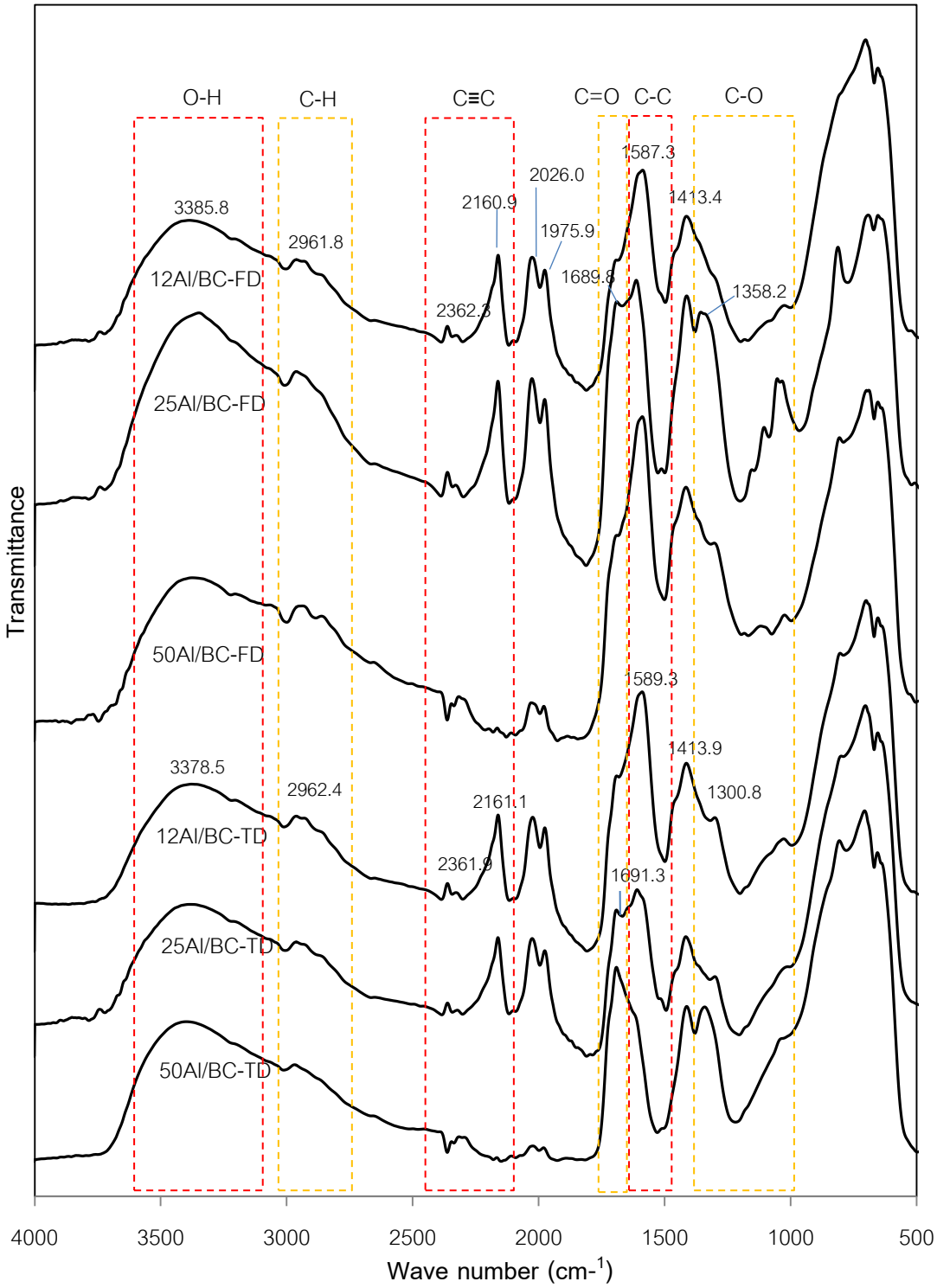

Figure 5.10 The FT-IR spectra of BC supported alumina catalysts in wave number ranging from 500 – 4000 cm^{-1}.

FT-IR spectroscopy has often been utilized as a useful tool in determination of functional groups or chemical bonds existing in a material [61]. **Figure 5.10** demonstrated the FT-IR spectra of BC supported alumina catalysts with various concentrations of Al loading and different dehydration conditions.

The FT-IR spectra of all catalyst samples were detected at wave number ranging from 4000 - 500 cm^{-1}. It was shown that the FTIR patterns of BC supported alumina catalysts dehydrated by hot air-drying were quite similar to those of BC supported alumina catalyst dehydrated by freeze-drying, considering at the same concentration of aluminium nitrate soaking solution. The broad band located around 3380 cm^{-1} is could be attributed to the O-H stretching vibration of hydroxyl group as hydrogen bonded-OH group. The band at 2962 cm^{-1} is related to C-H interaction with carbon surface. The sharp bands located at 2362 and 2161 cm^{-1} are attributed to the C≡C stretching vibration of alkyne group. However, those bands were not well observed in 50Al/BC-TD and 50Al/BC-FD. There is the band at 1690 cm^{-1}, which can be denoted as stretching C=O carbonyl groups. Moreover, the band at around 1670 to 1587cm^{-1} may be attributed to the C-C stretching vibration of aromatic ring and/or C=O of carboxylic group. In the region at around 1413 to 1300 cm^{-1} may relate to C-O stretching vibration. Consequently, the presence of oxygen surface functional group can be associated with the total acidity. The result from IR spectra indicated that the BC supported alumina catalysts were acid carbon catalysts, which were consistent with the values of total acidity obtained by acid-base back titration.

5.1.6. Thermal gravimetric analysis and differential thermal analysis (TGA/DTA)

Thermal decomposition of BC and BC supported alumina catalysts is observed by using TGA/DTA technique under air atmosphere in which is shown in **Figure 5.11 – 5.14**. The mass loss during the thermogravimetric analysis can be divided into three stages. **Figure 5.12(a) – 5.12(c)** show the TGA and DTA curves of BC supported alumina catalysts with various concentrations of Al loading dehydrated by hot air-drying. In the first stage, the weight loss occurs at temperature below 200 °C which could be attributed to moisture elimination. The second stage is found at temperature range about 200 °C to 400 °C indicating the volatilization of organic molecule. In the third stage, the weight loss occurs at temperature above 400 °C, which may be attributed to thermal decomposition and reaction between activating agent and carbonaceous residue.

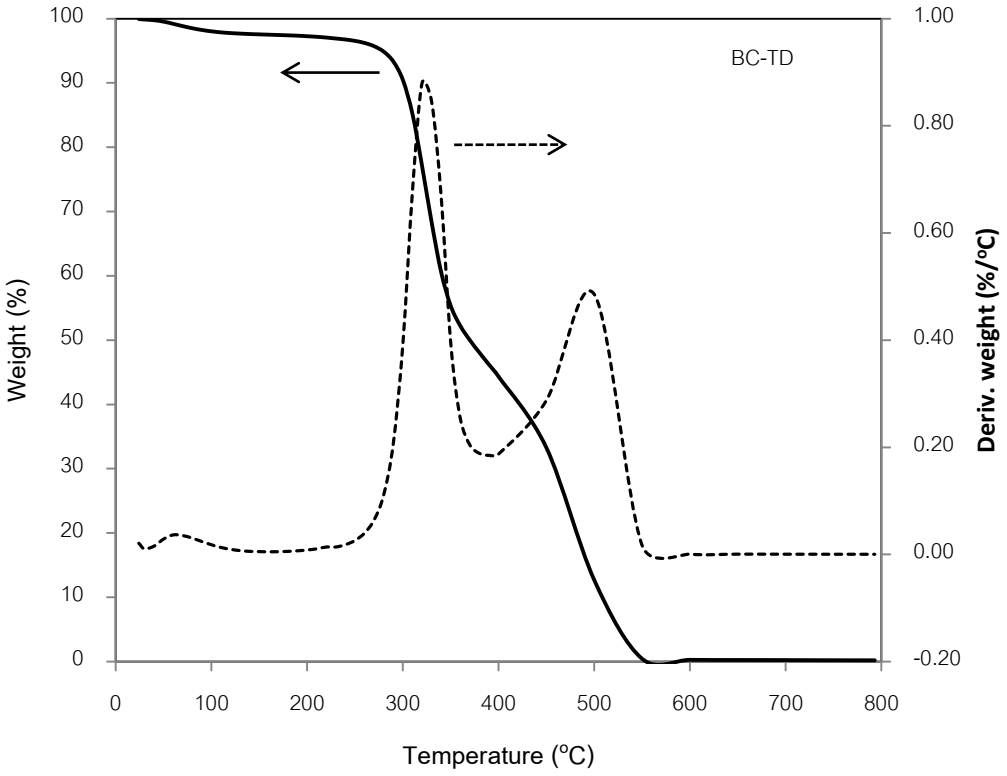

Figure 5.11 Thermal analysis of BC sample dehydrated by hot air-drying under air.

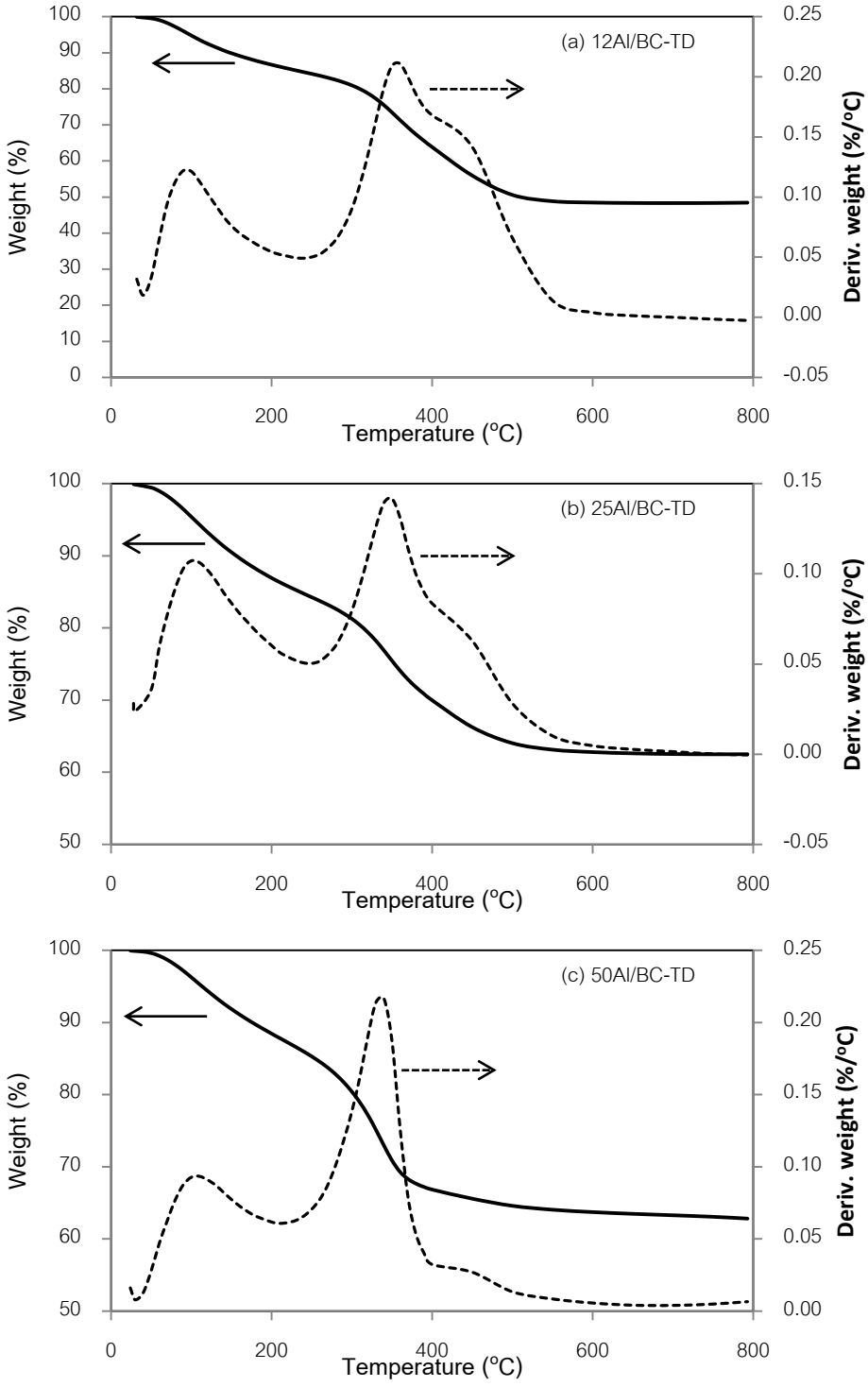

Figure 5.12 Thermal analysis of BC supported alumina catalysts dehydrated by hot air-drying under air.

Figure 5.14(a) – 5.14(c) show the TGA and DTA curves of BC supported alumina catalysts with various concentrations of Al loading dehydrated by freeze-drying that have the similar trend as of BC supported alumina catalysts dehydrated by hot air-drying.

When comparing between BC and BC supported alumina catalysts with 12, 25 and 50 %wt of Al loading both of dehydrating by hot air-drying and freeze-drying, the weight loss of BC supported alumina catalysts was less than that of BC, significantly. It indicated that Al loading on BC support had advantage as contribute to improvement of thermal stability in comparison with no Al loading BC as observed by TGA result.

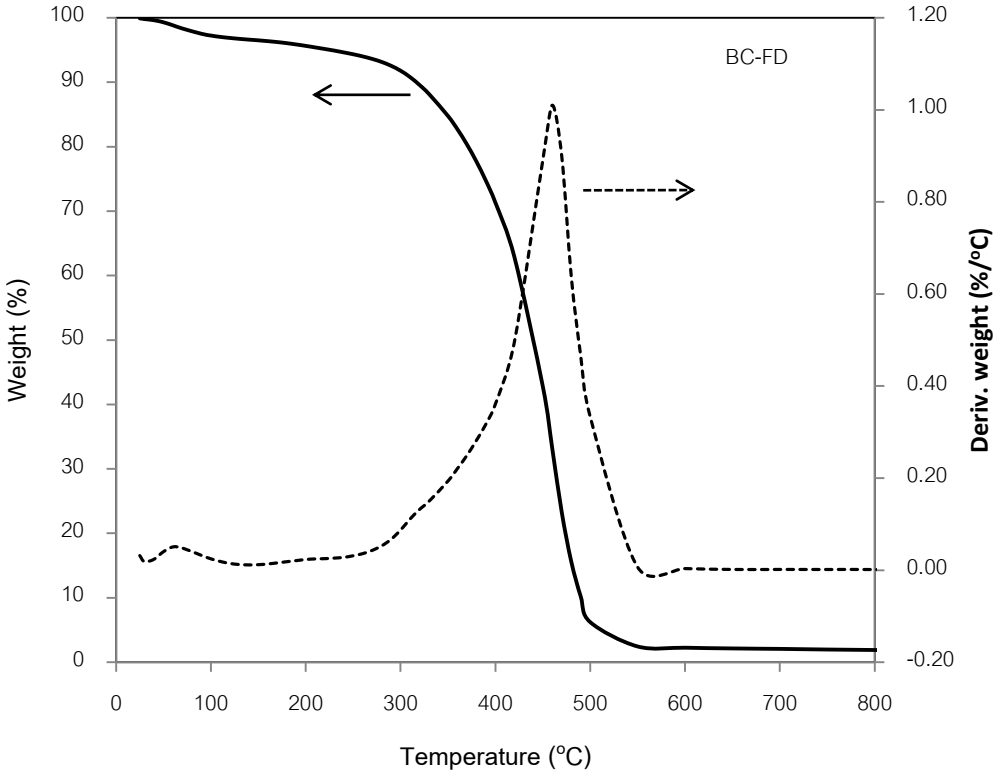

Figure 5.13 Thermal analysis of BC sample dehydrated by freeze-drying under air.

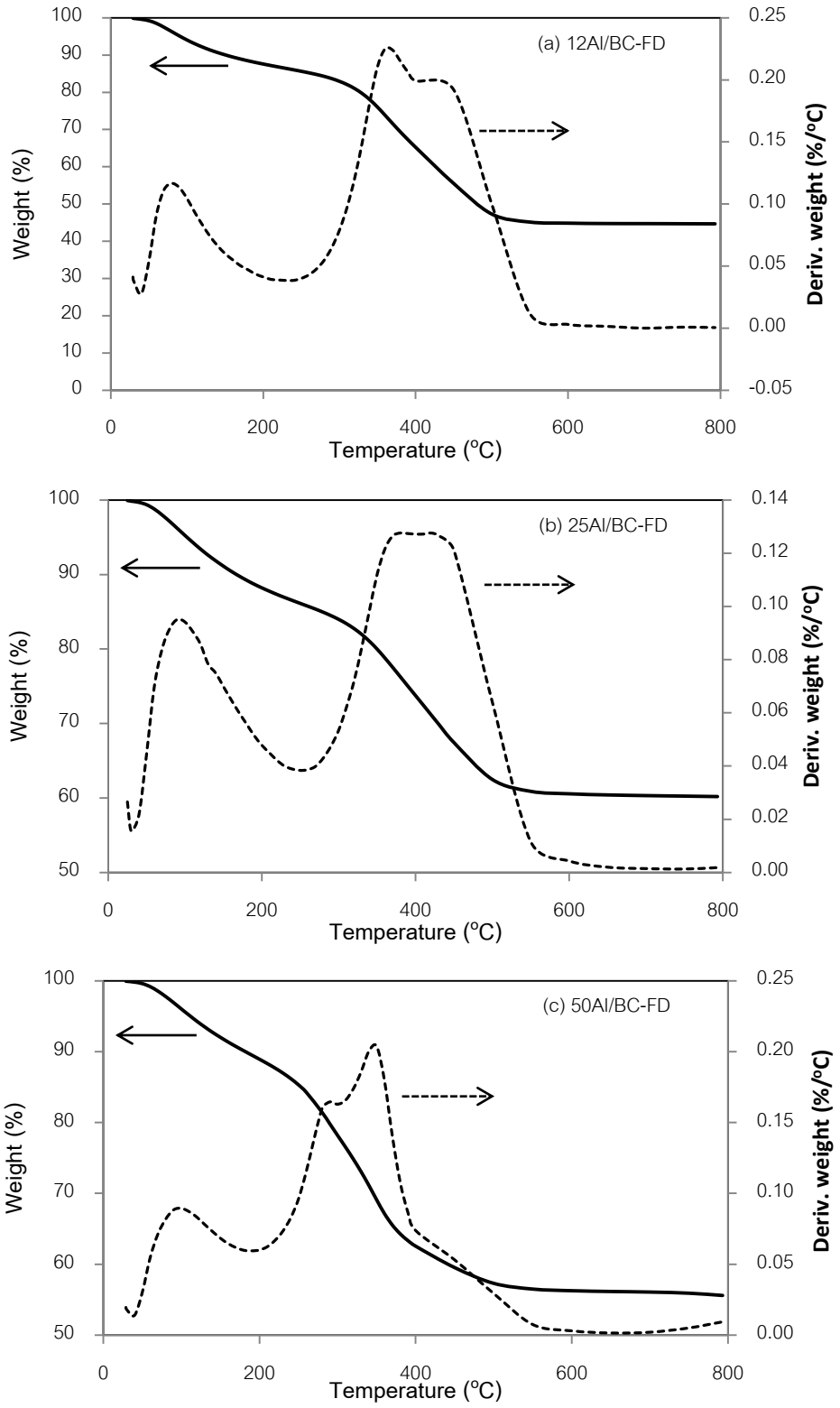

Figure 5.14 Thermal analysis of BC supported alumina catalysts dehydrated by freeze-drying under air.

5.2. Comparison of catalytic activity among BC supported alumina catalysts for ethanol dehydration

5.2.1. Catalytic activity

The catalyst performance of BC supported alumina catalysts were tested in ethanol dehydration reaction. First, 0.05 g of catalyst was packed into the fixed bed reactor, and then gas phase ethanol having flowrate of 50 ml/min was flowed into the reactor. The reaction was carried out in the temperature in the range of 200 ^{o}C to 400 ^{o}C.

The catalyst activity depends on the reaction temperature, according to previous reports [30, 50]. The results of catalytic activity were reported in term of selectivity and conversion versus temperature profile. The selectivity of ethylene, diethyl-ether, and acetaldehyde and ethanol conversion of all catalysts are shown in **Figures 5.15 – 5.18**. The ethylene formation is favored at high temperature which is endothermic reaction while the diethyl-ether is occurred at low temperature because of its exothermic reaction. Besides, acetaldehyde is byproduct which is formed at high temperature.

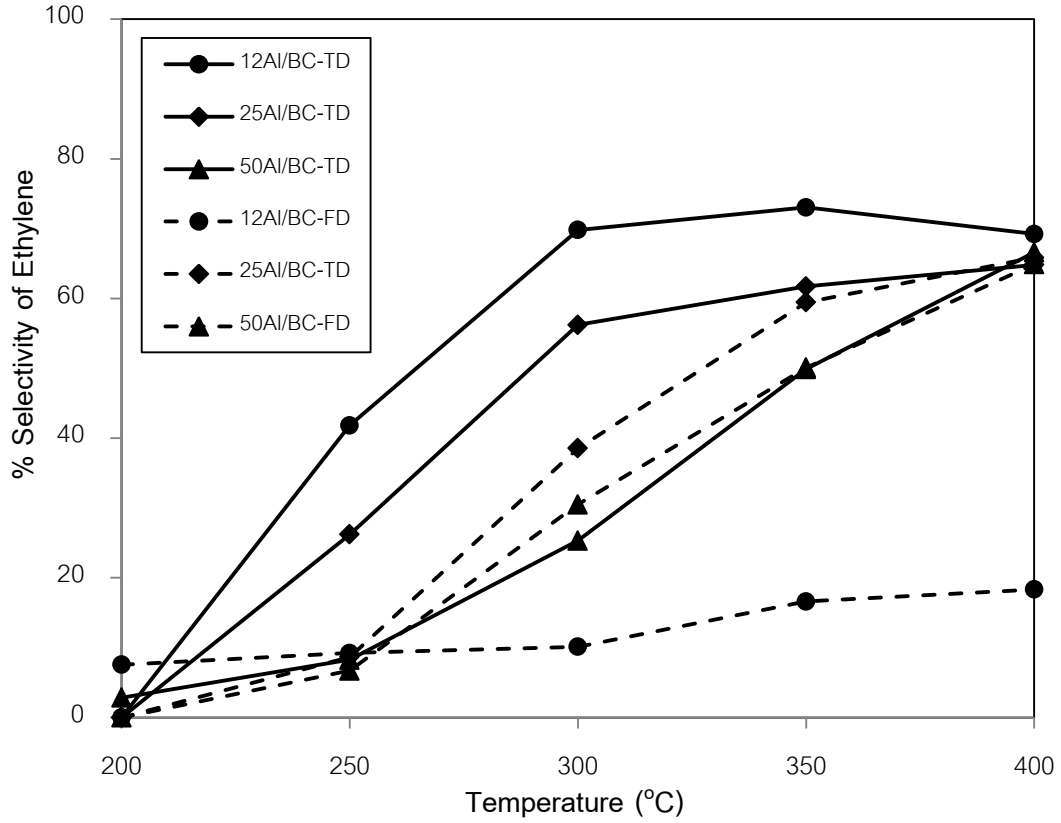

Figure 5.15 Selectivity of ethylene in ethanol dehydration of BC supported alumina catalysts at different temperatures.

Figure 5.15 displays the selectivity of ethylene over BC supported alumina catalysts at different temperatures. The result showed that at the reaction temperatures of 250 to 350 °C, the selectivity of ethylene was decreased with an increase of Al loading, which was in the order of 12Al/BC-TD > 25Al/BC-TD > 25Al/BC-FD > 50Al/BC-TD ~ 50Al/BC-FD. However, at the reaction temperature of 400 °C, all BC supported alumina catalysts showed quite similar selectivity of ethylene at about 64 to 69 % excepted for 12Al/BC-FD, which showed the lowest ethylene selectivity because of its low acidity. In addition, BC supported alumina catalysts dehydrated by hot air-drying obtained selectivity of ethylene relatively higher than those of BC supported alumina catalysts dehydrated by freeze-drying when considered at the same amount of Al

loading. Overall, the selectivity of ethylene increased with increasing reaction temperature because the reaction for ethylene production is endothermic reaction, which was opposite to that of the selectivity of diethyl-ether. For the selectivity of ethylene, the 12Al/BC-TD catalyst exhibited the highest selectivity (73.04 %) at 350 °C.

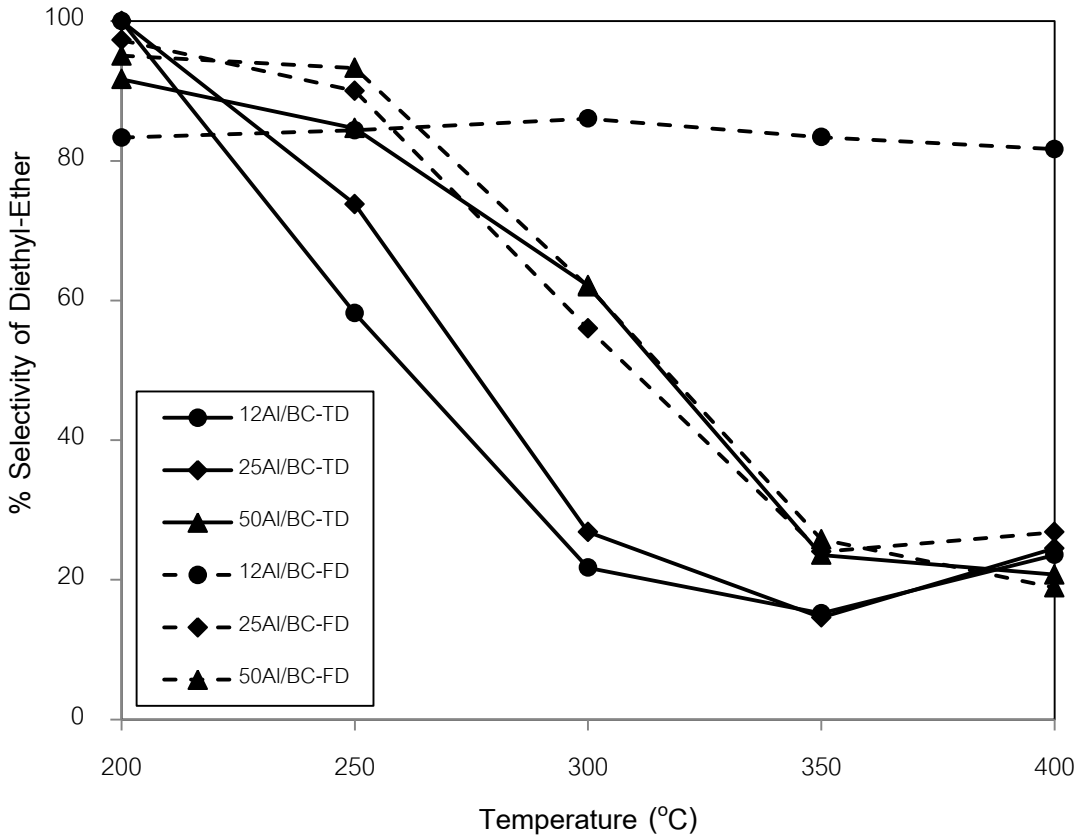

Figure 5.16 Selectivity of diethyl-ether in ethanol dehydration of BC supported alumina catalysts at different temperatures.

Figure 5.16 presents the selectivity of diethyl-ether, by product of ethanol dehydration reaction, over BC supported alumina catalysts at different temperatures. The selectivity of diethyl-ether was increased with an increase of Al loading. Moreover, BC supported alumina catalysts dehydrated by freeze-drying obtained selectivity of ethylene higher than those of hot air-drying, considering at the same amount of Al

loading. The results were in the order of 50Al/BC-FD > 25Al/BC-FD > 50Al/BC-TD > 25Al/BC-TD > 12Al/BC-TD at the reaction temperature in the range of 250 °C to 350 °C, excepted for 12Al/BC-FD, which showed the constant selectivity of diethyl-ether at all reaction temperatures. Overall, the selectivity of diethyl-ether significantly decreased with increasing reaction temperature because of its exothermic reaction. The highest selectivity of diethyl-ether was occurred at the reaction temperature of 200 °C.

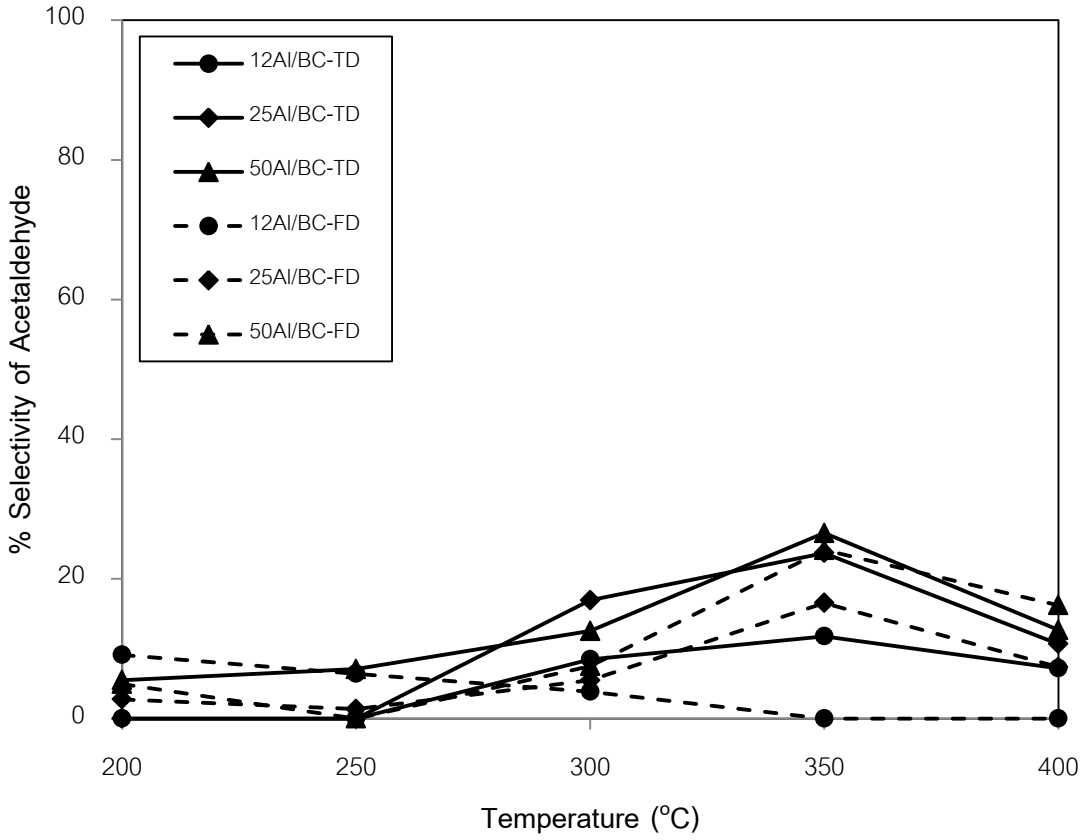

Figure 5. 17 Selectivity of acetaldehyde in ethanol dehydration of BC supported alumina catalysts at different temperatures.

Figure 5.17 presents the selectivity of acetaldehyde over BC supported alumina catalysts at different temperatures. The overall result showed that the selectivity of

acetaldehyde was increased with increasing reaction temperature, which was similar from that of the selectivity of ethylene.

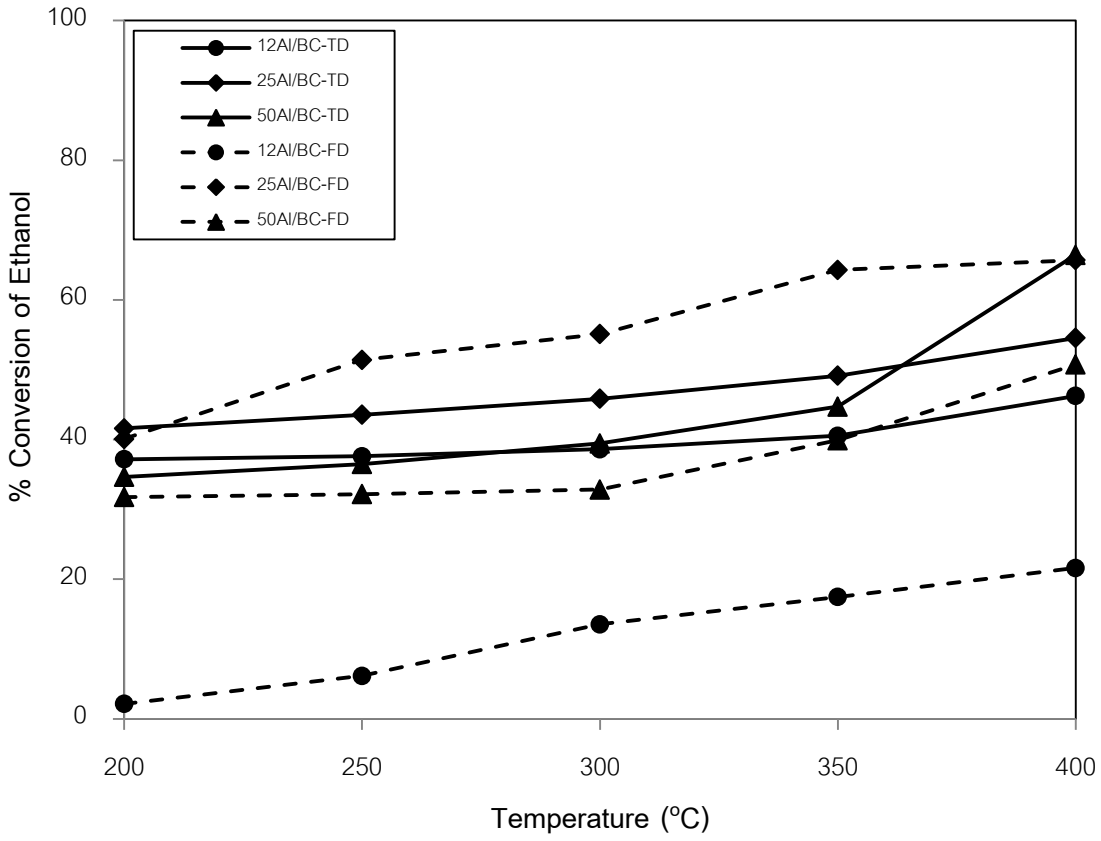

Figure 5.18 Ethanol conversion in ethanol dehydration of BC supported alumina catalysts at different temperatures.

The ethanol conversion over different catalysts is shown in **Figure 5.18**. The result showed that the ethanol conversion increasing with an increase in the reaction temperature. The ethanol conversion was in order of 25Al/BC-FD > 25Al/BC-TD > 12Al/BC-TD > 50Al/BC-TD > 50Al/BC-FD >12Al/BC-FD at the temperature in the range

of 250 °C to 300 °C. However, at 350 °C, the conversion of 50Al/BC-TD and 50Al/BC-FD raised up over that of 12Al/BC-TD and finally, at the temperature of 400 °C, the ethanol conversion became in the order of 50Al/BC-TD > 25Al/BC-FD > 25Al/BC-TD > 50Al/BC-FD > 12Al/BC-TD > 12Al/BC-FD. The highest ethanol conversion at 66.43 % with ethylene selectivity at 66.60 % was obtained with the use of 50Al/BC-TD at the reaction temperature of 400 °C. Although 50Al/BC-TD gives the best ethanol conversion at 400 °C, 25Al/BC-FD also provides relatively similar conversion to that of 50Al/BC-TD. In addition, the advantages of 25Al/BC-FD over 50Al/BC-TD include 1) less chemicals and energy requirement for the preparation and 2) much higher ethanol conversion at low temperature (200 °C to 350 °C). Consequently, 25Al/BC-FD is considered as the more attractive catalyst than 50Al/BC-TD for utilization in industry.

The catalytic activity of all BC supported alumina catalysts in term of selectivity of ethylene, diethyl-ether, and acetaldehyde and ethanol conversion is summarized as shown in **Table 5.4**.

Table 5.4 Comparison of catalyst activity of BC supported alumina catalysts at optimum temperature of 400 ^{o}C.

Catalyst Sample	% Selectivity of Ethylene	% Selectivity of diethyl-ether	% Selectivity of acetaldehyde	% Conversion of ethanol
12Al/BC-TD	69.24	23.57	7.19	46.24
25Al/BC-TD	64.83	24.50	10.67	54.55
50Al/BC-TD	66.60	20.73	12.67	66.43
12Al/BC-FD	18.33	81.67	0.00	21.62
25Al/BC-FD	65.84	26.82	7.34	65.70
50Al/BC-FD	64.91	18.86	16.21	50.74

Considering at the same reaction temperature, it was observed that the acidity plays an important role in ethanol conversion and ethylene selectivity. In addition, surface area of catalyst also had an effect on catalytic activity. Higher surface area resulted in an increase in ethanol conversion.

5.2.2. Comparison of catalyst activity of BC supported alumina catalysts with other catalysts in ethanol dehydration at reaction temperature of 400 °C

Table 5.5 shows the catalytic activity of other catalysts in ethanol dehydration for comparison with BC supported alumina catalysts at the reaction temperature of 400 °C.

Table 5.5 Comparison of catalyst activity of BC supported alumina catalysts with other catalysts in ethanol dehydration at reaction temperature of 400 °C.

Catalyst Sample	Authors	% Selectivity of ethylene	% Selectivity of diethyl-ether	% Selectivity of acetaldehyde	% Conversion of ethanol
50Al/BC-TD	This work	66.60	20.73	12.67	66.43
25Al/BC-FD	This work	65.84	26.82	7.34	65.70
H_2SO_4/ACC	Lamphun *et al.* (2014)	19	0	81	37
H_2SO_4/Dry_AC 400 (derived from BC)	Lamphun *et al.* (2014)	80	14	6	85
C50_600 (Alumina)	Tharmmanoon *et al.* (2013)	95	1	4	100
60Al_SSP (Alumina-silica)	Titinan *et al.* (2013)	95	5	0	100
5%Ni/ACC	Somrudee *et al.* (2013)	15	5	80	45

By being compared to H_2SO_4/Dry_AC 400, catalysts prepared from activated carbon derived from BC and impregnated with sulfuric acid, 50Al/BC-TD and 25Al/BC-FD render lower ethylene selectivity and ethanol conversion due to lower acidity and surface area. Compared to alumina catalysts using other supports, such as C50_600

and 60Al_SSP, the Al/BC catalysts also show lower catalytic activity because of less surface area. However, the Al/BC catalysts are quite attractive for industrial application because they require much lower calcination temperature and use only a small amount of chemicals with much simpler preparing method. Moreover, the Al/BC catalysts prepared in this work have higher catalytic activity than H_2SO_4/ACC (commercial grade activated carbon) and 5%Ni/ACC for production of ethylene by ethanol dehydration.

CHAPTER VI

CONCLUSIONS AND RECOMMENDATIONS

This chapter draws conclusion of the experimental results, which comprised characteristic and catalytic activity of BC supported alumina catalysts with various concentrations of Al loading and different dehydrating conditions for ethanol dehydration. These are described in section 6.1. Moreover, section 6.2 mentioned recommendations for future study.

6.1 Conclusions

1. The BC and BC supported alumina catalysts in this work are presented of mesoporous structure ranging from 8.917 nm to 34.250 nm in average pore diameter.

2. Increase in Al loading on BC supported alumina catalyst resulted in decreasing of surface area with increased average pore diameter.

3. BC supported alumina catalysts dehydrated by freeze-drying method has higher BET surface area and pore volume than those of hot air-drying method, but comparable pore diameter at the same amount of Al loading.

4. 25Al/BC-FD catalyst which is referred to BC supported alumina catalyst with 25 %wt alumina loading dehydrated by freeze drying exhibits the highest surface area and total pore volume, which are 21.920 m^2/g and 0.1439 cm^3/g, respectively.

5. The distribution of alumina on BC support is uniform and well dispersion.

6. Increase in Al loading resulted in increasing of acidity property but decreasing of crystalline structure.

7. It was found that the BC supported alumina catalysts was effective for the use as the catalyst in ethanol dehydration, which produced ethylene as the main product. The highest ethanol conversion at 66.43 % with ethylene selectivity of 66.60 % was obtained by the use of 50Al/BC-TD catalyst at reaction temperature of 400 ^{o}C.

8. Al loading on BC support had advantage as contribute to improvement of thermal stability in comparison with Al unloading BC as indicated by TGA.

6.2 Recommendations

1. Other properties of BC supported alumina catalyst such as life span, acidity test by NH_3-TPD, time on stream (stability test), and etc. should be further investigation.

2. Other acidic metals impregnated onto the BC support should be investigated for enhanced catalytic performance at low temperature.

3. Other calcination temperatures of BC supported alumina catalysts above 200 ^{o}C should be further investigated in order to obtain suitable acidity property and crystalline structure of metal oxide.

4. Deactivation of the catalyst at difference reaction temperature should be investigated in order to improve this catalyst for utilization in industry.

REFERENCES

1. Giuseppe, S., *Mechanical Properties of Bacterial Cellulose Implants.* Technical report, 2010. **n.366**: p. 7-8.
2. Pretre, G., P. Zarnea, and E. Adrian, *Biodegradation and bioconversion of cellulose waste using bacterial and fungal cells immobilized in radio polymerized hydrogels.* Conservation and Recycling, 1999. **27** p. 309-332.
3. Saied, H.E., A.H. Basta, and R.H. Gobran, *Research Progress in Friendly Environmental Technology for the Production of Cellulose Products (Bacterial Cellulose and Its Application).* Polymer-Plastics Technology and Engineering, 2004 **43**(3): p. 797-820.
4. Jonas, R. and L.F. Farah, *Production and application of microbial cellulose.* Polymer degradation and Stability, 1998 **59** p. 101-106.
5. Budhionoa, A., et al., *Kinetic aspects of bacterial cellulose formation in nata-de-coco culture.* Carbohydrate Polymers, 1999. **40**: p. 137-143.
6. Yamamoto, H., F. Horii, and H. Odani, *Structural changes of native cellulose crystals induced by annealing in aqueous alkaline and acidic solutions at high temperatures.* Macromolecules, 1989: p. 4130-4132.
7. Fontana, J.D., et al., *Acetobactor cellulose pellicle as a temporary skin substitute.* Applied Biochemistry and Biotechnology, 1990. **24/25**: p. 253-263.
8. Klemm, D., et al., *Bacterial synthesized cellulose artificial blood vessels for microsurgery.* Progress in Polymer Science, 2001 **26** p. 1561-1603.
9. Svensson, A., et al., *Bacterial cellulose as a potential scaffold for tissue engineering of cartilage.* Biomaterials, 2005. **26**: p. 419-431.
10. Czaja, W., A. Krystynowicz, and S. Bielecki, *Microbial cellulose-the natural power to heal wounds.* Biomaterials, 2006. **27**: p. 145-151.
11. Klemm, D., et al., *Cellulose: Fascinating biopolymer and sustainable raw material.* Angew. Chem., Int. Ed., 2005 **44(22)**: p. 3358.

12. Xu, Y., L. Zhang, and Y. Cu, *Catalytic performance of cellulose supported palladium complex for Heck reaction in water.* J. Appl. Polym. Sci., 2008. **110**: p. 2996.

13. Yang, J.Z., et al., *Biotemplated preparation of CdS nanoparticles/bacterial cellulose hybrid nanofibers for photocatalysis application.* J. Hazard. Mater, 2011. **189**(1-2): p. 377.

14. Bedia, J., et al., *Ethanol dehydration to ethylene on acid carbon catalysts.* Applied Catalyst B: Enviromental, 2011. **103**: p. 302-310.

15. Denise, F., D. Der-Jong, and W. Ho-Shing, *Ethylene formation by catalytic dehydration of ethylene with industrial consideration.* Materials, 2013. **6**: p. 101-115.

16. Huang, L.D., *Ethylene and its industry status.* China Chlor-Alkali, 2005. **5(5)**: p. 1-5.

17. Minhua, Z. and Y. Yingzhe, *Dehydration of ethanol to ethylene.* Ind. Eng. Chem. Res., 2013 **52**: p. 9505-9514.

18. Zotov, R.A., et al., *Characterization of the active sites on the surface of Al_2O_3 ethanol dehydration catalysts by EPR using spin probes.* Journal of Catalysis, 2011. **278**: p. 71-77.

19. Okagami, A. and S. Matsuoka, *Process for manufacturing olefins by catalytic oxidation of hydrocarbons.* US patent 3541179, 1970. **11**: p. 07.

20. Wang, S.H. and X.O. He, *Ethylene process and technology.* China Petrochemical Press: Beijing, 2000.

21. Koyama, J., T. Sugiyama, and Itoh, *Systematic survey on crystalline features of algal cellulose.* Cellulose, 1997 p. 147-160.

22. Gardner, K.H. and J. Blackwell, *The structure of native cellulose.* Biopolymer, 1974. **13**: p. 1975-2001.

23. Schramm, M., Z. Grommet, and S. Hestrin, *Synthesis of cellulose by Acetobacter xylinum.* Substrates and Inhibitors Biochemical, 1957 **67**: p. 669-679.

24. Brown, J.P.M., *Advances in cellulose biosynthesis polymers from biobased materials.* New Jersey: Prentice hall, 1991.

25. Sangrungraungroj, W., *Development ofr celloulose membrane from nata-de-coco for material separation*, in *Department of chemical engineering, Faculty of Engineering*. 2003, Chulalongkorn University.

26. Suwanmajo, T., *Development of nanostructure membrane from regenerated bacterial cellulose*, in *Department of chemical engineering, Faculty of engineering* 2006, Chulalongkorn University

27. Sani, A. and Y. Dahman, *Improvements in the production of bacterial synthesized biocellulose nanofibres using different culture methods.* J Chem Tech Biotechnol, 2010. **85** (2): p. 151-164.

28. Olaf, W. and E. Meng-Teck, *Make ethylene from ethanol.* Hydrocarbon Process, 1976 **55** (11): p. 125-133.

29. Isao, T., et al., *Dehydration of ethanol into ethylene over solid acid catalysts.* Catalysis Letters, 2005. **105**: p. 3-4.

30. Lu, J., Y. Liu, and N. Li, *Fe-modified HZSM-5 catalysts for ethanol conversion into light olefins.* Natural Gas Chemistry, 2011 **20** p. 423–427.

31. Joseph, F., et al., *Kinetics and mechanism of ethanol dehydration on γ-Al2O3: The critical role of dimer inhibition.* Catalysis Letters, 2013 **3** p. 798-807.

32. Vijai, V.B. and D.Y. Ganapati, *Heteropolyacid supported on montmorillonite catalyst for dehydration of dilute bio-ethanol.* Applied Clay Science, 2011. **53** p. 263-271.

33. Varisli, D., T. Dogu, and G. Dogu, *Ethylene and diethyl-ether production by dehydration reaction of ethanol over different heteropolyacid catalysts.* Chem. Eng. Sci., 2007. **62**: p. 5349-5352.

34. Chen, G., et al., *Catalysts in microchannel reactors.* Catal. Today, 2007. **125**: p. 111-119.

35. Izabela, N. and Z. Maria, *Niobium compounds: Preparation, characterization, and application in heterogeneous catalyst.* Chem. Rev, 1999. **99** p. 3603-3624.

36. Wade, L.G., Jr.,, *Organic Chemistry*. Fifth Edition ed. 2003, Prentice-Hall, Saddle River, NJ.

37. Alvin, B.S., *Catalyst supports and supported catalyst-theoretical and applied concepts.* 1987.

38. Karen, D., *Material review: alumina (Al_2O_3)*. 2010 School of Doctoral Studies (European Union) Journal.

39. Khom-in, J., *Synthesis of dimethylether (DME) from dehydration of methanol using γ-Al_2O_3 and γ-x-Al_2O_3 catalyst*, in *Master's thesis, Department of chemical engineering, Faculty of Engineering*. 2007, Chulalongkorn University.

40. Thamonwan, J. and J. Bunjerd, *Carbon dioxide hydrogenation over alumina-silica composite-supported cobalt catalyst*, in *Chemical Engineering* 2010, Chulalongkorn University.

41. Daniell, W., et al., *Enhanced surface acidity in mixed alumina-silicas: a low temperature FTIR study.* Applied Catalysis A: General, 2000. **196**: p. 247-260.

42. Elio, S., G. Davlno, and C. Sergio, *Basic behavior of alumina in the presence of strong acids.* Ind. Eng. Chem. Prod. Res. Dev, 1977. **16**(1): p. 45-47.

43. Iguchi, M., S. Yamanaka, and Budhiono A., *Bacterial cellulose – a masterpiece of nature's arts.* J Master Sci, 2000: p. 261-270.

44. Hiroshi, O., et al., *Emulsion-stabilization effect of Bacterial Cellulose.* Biosci Biotechnol and Biochem, 1997: p. 1541-1545.

45. Peipei, Z., et al., *Bacteria cellulose nanofibers supported palladium(0) nanocomposite and its catalysis evaluation in Heck reaction.* Ind. Eng. Chem. Res. , 2012 **51** p. 5743-5748.

46. Jiazhi, Y., et al., *Biotemplated preparation of CdS nanoparticles/BC hybrid nanofibers for photocatalysis application.* Journal of Hazardous Materials, 2011 **189** p. 377–383.

47. Pan, L.R., *Development review of catalysts for ethanol dehydration to produce ethylene.* Speciality Petrochem, 1986 **4**: p. 41-64.

48. Pearson, D.E., et al., *Phosphoric acid system catalytic conversion of fermentation ethanol to ethylene.* Prod. Res. Dev. , 1981 **20**(4): p. 734–740.

49. Madeira, F.F., et al., *Ethanol transformation over HFAU, HBEA and HMFI zeolites presenting similar BrØnsted acidity.* Appl. Catal. A, 2009. **367**: p. 39-46.

50. Ouyang, J., et al., *Catalytic conversion of bioethanol to ethylene over La-modified HZSM-5 catalysts in a bioreactor.* Catalysis Letters, 2009 **132** p. 64-74.

51. Takahashi, A., et al., *Effects of added phosphorus on conversion of ethanol to propylene over ZSM-5 catalysts.* Applied Catalysis A: General, 2012: p. 162–167.

52. Zhang, D., R. Wang, and X. Yang, *Effect of P content on the catalytic performance of P-modified HZSM-5 catalysts in dehydration of ethanol to ethylene.* Catal. Lett. , 2008. **124**: p. 384-391.

53. Leandro, M., et al., *Efficiency of ethanol conversion induced by controlled modification of pore structure and acidic properties of alumina catalysts.* Applied Catalysis A: General, 2011 **398** p. 59–65.

54. Ying, X., Z. Lei, and C. Yuanchen, *Catalytic performance of cellulose supported palladium complex for heck reaction in water.* Wiley InterScience, 2008.

55. Jamwal, N., et al., *Nano Pd(0) supported on cellulose: A highly efficient and recyclable heterogeneous catalyst for the Suzuki coupling and aerobic oxidation of benzyl alcohols under liquid phase catalysis.* International Journal of Biological Macromolecules, 2011. **49** p. 930–935.

56. Sajjad, K., S. Salman, and S. Ahmad, *Palladium nano-particles supported on ethylenediaminefunctionalized cellulose as a novel and efficient catalyst for the Heck and Sonogashira couplings in water.* Cellulose, 2013. **20**: p. 973-980.

57. Heeyeon, K., J. Nam, and O. Seong, *Synthesis of a catalytic support from natural cellulose fibers, and its performance in a CO_2 reforming of CH_4.* Applied Catalysis B: Environmental, 2012. **113-114** p. 116-125.

58. Phisalaphong, M., T. Suwanmajo, and P. Sangtherapitikul, *Novel nanoporous membranes from regenerated bacterial cellulose.* Journal of Applied Polymer Science, 2008 **107** p. 292–299.

59. Kitano, M., et al., *Preparation of a sulfonated porous carbon catalyst with high specific area.* Catal Lett, 2014. **131**: p. 242-249.

60. Xiang, Q., et al., *Heterogeneous aspects of acid hydrolysis of α-cellulose.* Applied Biochemistry and Biotechnology, 2003. **505**: p. 105-108.

61. Lee, Y.M., S.H. Kim, and S.J. Kim, *Preparation and characterization of β-chitin and poly (vinyl alcohol) blend.* Polymer, 1994 **37**: p. 5897-5905.

APPENDIX

APPENDIX A

CALCULATION OF CONVERSION AND SELECTIVITY

This research studied the catalyst performance by used ethanol dehydration reaction. Consider in term of ethanol conversion and selectivity.

Ethanol Conversion

The ethanol conversion is described that mole of ethanol converted with respect to ethanol in feed as follow:

$$\text{Ethanol convertion (\%)} = \frac{\text{mole of ethanol in feed} - \text{mole of ethanol in product X 100}}{\text{mole of ethanol in feed}}$$

Selectivity

The selectivity of this product is described by mole ratio of a specific product to main products formed such as acetaldehyde, ethylene and di-ethyl ether) as follow:

$$\text{Selectivity of A (\%)} = \frac{\text{mole of A formed } X \text{ 100}}{\text{mole of total product}}$$

Where A is mole of ethylene, diethyl-ether, or acetaldehyde

Total product is mole of ethylene + diethyl-ether + acetaldehyde

APPENDIX B

POROSITY AND SORPTION BEHAVIOUR

(Refer: http://personal.strath.ac.uk/ashleigh.fletcher/adsorption.htm)

Classification of pores

Porosity has a classification system as defined by IUPAC, which gives a guideline of pore widths applicable to all forms of porosity. Distinctions in porosity class are not rigorous and they may often overlap in size and definition. The widely accepted IUPAC classification is as follows:

- Micropores width less than 2 nm
- Mesopores width between 2 and 50 nm
- Macropores width greater than 50 nm

Microporosity may then be subdivided into three subsequent categories:

- Ultramicropores width less than 0.5 nm
- Micropores width between 0.5 - 1.4 nm
- Supermicropores width between 1.4 - 2.0 nm

Classification of adsorption isotherms

All adsorption isotherms should fit at least one, or at least a combination of two or more, of the six recognized types classified by Brunauer, Deming, Deming and Teller (B.D.D.T. system). The figure above shows the possible shapes and information which may be drawn from them is outlined below:

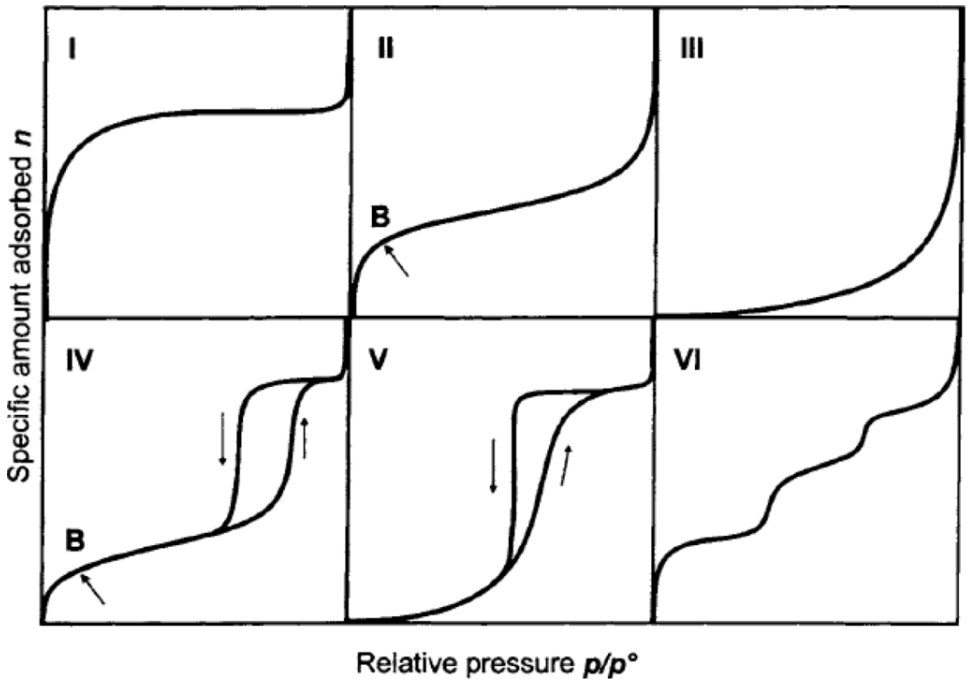

Diagrammatic Representation of Isotherm Classification

Type I Isotherm - these are typical of adsorbents with a predominantly microporous structure, as the majority of micropore filling will occur at relative pressures below 0.1. The adsorption process is usually complete at a partial pressure of ~0.5. Examples include the adsorption of nitrogen on carbon at 77K and ammonia on charcoal at 273K.

Type II Isotherm - physical adsorption of gases by non-porous solids is typified by this class of isotherm. Monolayer coverage is followed by multi-layering at high relative pressures. Carbons with mixed micro- and mesoporosity produce Type II isotherms.

Type III Isotherm - the plot obtained is convex to the relative pressure axis. This class of isotherm is characteristic of weak adsorbate-adsorbent interactions and is most commonly associated with both non-porous and microporous adsorbents. The weak interactions between the adsorbate and the adsorbent lead to low uptakes at low relative pressures. However, once a molecule has become adsorbed at a primary adsorption site, the adsorbate-adsorbate interaction, which is much stronger, becomes the driving force of the adsorption process, resulting in accelerated uptakes at higher relative pressure. This co-operative type of adsorption at high partial pressures is known as cluster theory and examples include the adsorption of water molecules on carbon where the primary adsorption sites are oxygen based.

Type IV Isotherm - A hysteresis loop, which is commonly associated with the presence of mesoporosity, is a common feature of Type IV isotherms, the shape of which is unique to each adsorption system. Capillary condensation gives rise to a hysteresis loop and these isotherms also exhibit a limited uptake at high relative pressures.

Type V Isotherm - these isotherms are convex to the relative pressure axis and are characteristic of weak adsorbate-adsorbent interactions. These isotherms are indicative of microporous or mesoporous solids. The reasons behind the shape of this class of isotherm are the same as those for Type III and again water adsorption on carbon may exhibit a Type V isotherm.

Type VI Isotherm - introduced primarily as a hypothetical isotherm, the shape is due to the complete formation of monomolecular layers before progression to a subsequent layer. It has been proposed, by Halsey that the isotherms arise from adsorption on extremely homogeneous, non-porous surfaces where the monolayer capacity corresponds to the step height. One example known to exist is the adsorption of krypton on carbon black (graphitized at 3000 K) at 90 K.

VITA

Mr. Miftahfarid Ibnu Abdulwahab was born in Narathiwat, Thailand. He received the degree of Bachelor of Engineering in Chemical Engineering from the School of Chemical Engineering, Institute of Engineering, Suranaree University of Technology in August 2005. He entered the Master of Engineering Program in Chemical Engineering at the Department of Chemical Engineering, Faculty of Engineering, Chulalongkorn University in June, 2012. During the program studying, he has been employed as a Strategic Project Engineer at Begemann Mercury Technology Pacific (BMTP) Co., Ltd.